View metadata, citation and similar papers at core.ac.uk

brought to you by CORE

provided by NASA Technical Reports Server

RESTRICTED SECURITY INFORMATION

JUN 22 1951

c. 2

ALD 4-27-53

NACA

RESEARCH MEMORANDUM

LOW-SPEED LONGITUDINAL AND WAKE AIR-FLOW CHARACTERISTICS AT A REYNOLDS NUMBER OF 5.5×10^6 OF A CIRCULAR-ARC 52° SWEPTBACK WING WITH A FUSELAGE AND A HORIZONTAL TAIL AT VARIOUS VERTICAL POSITIONS

By Gerald V. Foster and Roland F. Griner

Langley Aeronautical Laboratory
Langley Field, Va.

CLASSIFICATION CANCELLED
Authority NACA Res. 4-4-57 Date 3/16/58
RN 9 8
By NACA 4-24-57 Sec

CLASSIFICATION CHANGED
To
Rel. form H 1602
CLASSIFIED DOCUMENT
J. W. Crowley Date 12-1-53
This document contains classified information affecting the National Defense of the United States within the meaning of the Espionage Act, USC 50:31 and 32. Its transmission or the revelation of its contents in any manner to an unauthorized person is prohibited by law.
Information so classified may be imparted only to persons in the military and naval services of the United States, appropriate civilian officers and employees of the Federal Government who have a legitimate interest therein, and to United States citizens of known loyalty and discretion who of necessity must be informed thereof.
JH-12-10-53

NATIONAL ADVISORY COMMITTEE FOR AERONAUTICS

WASHINGTON

June 19, 1951

FOR REFERENCE

NOT TO BE TAKEN FROM THIS ROOM

NACA LIBRARY
LANGLEY AERONAUTICAL LABORATORY
Langley Field, Va.

RESTRICTED

CONFIDENTIAL SECURITY INFORMATION

NASA Technical Library
3 1176 01436 8550

CONFIDENTIAL
SECURITY INFORMATION

NATIONAL ADVISORY COMMITTEE FOR AERONAUTICS

RESEARCH MEMORANDUM

LOW-SPEED LONGITUDINAL AND WAKE AIR-FLOW CHARACTERISTICS AT A REYNOLDS NUMBER OF 5.5×10^6 OF A CIRCULAR-ARC 52° SWEPTBACK WING WITH A FUSELAGE AND A HORIZONTAL TAIL AT VARIOUS VERTICAL POSITIONS

By Gerald V. Foster and Roland F. Griner

SUMMARY

An investigation has been conducted in the Langley 19-foot pressure tunnel to determine the effects of a fuselage and a horizontal tail located at various vertical positions on the low-speed longitudinal characteristics of a circular-arc 52° sweptback wing. Air-flow surveys were made in a vertical plane at a position which corresponded approximately to the longitudinal location of the horizontal tail. The results were obtained at a Reynolds number of 5.5×10^6 with and without leading-edge and trailing-edge flaps.

The low tail (located 0.132 semispan below the wing-chord plane) was situated below the wake center for moderate and high angles of attack and had a stabilizing influence through the angle-of-attack range because of a favorable rate of change of downwash angle with angle of attack. The intermediate and high tails (located 0.136 and 0.442 semispan above the wing-chord plane) had a stabilizing influence at low angles of attack; however, at moderate and high angles of attack large increases in the rate of change of downwash with angle of attack cause a decrease in the stabilizing effect of these tails. The effect of the high tail actually became destabilizing at high angles of attack.

The most favorable improvements in dC_m/dC_L (rate of change of pitching-moment coefficient with lift coefficient) were obtained with the low and intermediate tails. Although all configurations with these tails were considerably out of trim at high angles of attack, an analysis indicated that the effects of trim would not appreciably change the stability realized with these tails. With either of these tails the change in static margin through the lift range might be undesirable.

[redacted]

[redacted] SECURITY INFORMATION

The 0.25-semispan leading-edge flaps increased the maximum lift coefficient, improved the stability of the wing-fuselage configuration in the high angle-of-attack range, and reduced the changes in dC_m/dC_L through the moderate angle-of-attack range with either the intermediate tail or low tail.

The addition of a fuselage to the wing resulted in an increase in maximum lift coefficient. With the fuselage on, some improvement was realized in the variation of dC_m/dC_L in the high angle-of-attack range of the 0.25-semispan leading-edge-flap configuration; however, in general, the effects of the fuselage on the stability of the wing were small.

The stabilizing contribution of the horizontal tail can be predicted with a fair degree of accuracy from the air-flow survey data.

INTRODUCTION

As part of a general study at the Langley 19-foot pressure tunnel to determine the effect of a horizontal tail on the longitudinal stability characteristics of swept wings, a low-speed investigation has been made of a 52° sweptback wing in combination with a fuselage and a horizontal tail. The wing had symmetrical circular-arc sections, an aspect ratio of 2.84, and a taper ratio of 0.616. The longitudinal characteristics of the wing alone, with and without leading-edge and trailing-edge flaps, are presented in reference 1.

This paper presents results which show the effects of a fuselage and a horizontal tail (at various vertical positions) on the longitudinal characteristics of the wing with and without leading-edge and trailing-edge flaps. Results are also included of air-flow surveys made behind the wing at a longitudinal location which corresponded approximately to the longitudinal location of the tail.

The data presented herein were obtained at a Reynolds number of 5.5×10^6 and a Mach number of 0.11.

SYMBOLS AND COEFFICIENTS

C_L lift coefficient $\left(\frac{\text{Lift}}{qS}\right)$

C_D drag coefficient $\left(\frac{\text{Drag}}{qS}\right)$

C_m pitching-moment coefficient, moment about $0.25\bar{c}$ $\left(\frac{\text{Moment}}{qS\bar{c}}\right)$

$\bar{c}$ mean aerodynamic chord (M.A.C.) measured parallel to the plane of symmetry, feet $\left(\frac{2}{S}\int_0^{b/2} c^2 dy\right)$

S area (wing unless otherwise noted), square feet

b span (wing unless otherwise noted), feet

c local chord (wing unless otherwise noted), feet

y spanwise ordinate, feet

q free-stream dynamic pressure, pounds per square foot $\left(\frac{1}{2}\rho V^2\right)$

ρ mass density of air, slugs per cubic foot

α angle of attack (of wing chord unless otherwise noted), degrees

V free-stream velocity, feet per second

q_t/q ratio of local dynamic pressure at horizontal tail to free-stream dynamic pressure (unless otherwise noted)

ϵ local downwash angle (unless otherwise noted), degrees

σ local sidewash angle (inflow negative), degrees

i_t angle of incidence of horizontal tail measured with respect to wing-chord plane, positive when trailing edge is down, degrees

τ tail stability parameter

T tail volume $\left(\frac{l}{\bar{c}}\frac{S_t}{S}\right)$

η tail efficiency factor, ratio of $\left(C_{m_{i_t}}\right)_o$ of any tail position to $\left(C_{m_{i_t}}\right)_o'$

$\frac{dC_m}{dC_L}$ rate of change of pitching-moment coefficient with lift coefficient

$\frac{dC_{m_t}}{d\alpha}$ rate of change of pitching-moment coefficient due to tail with angle of attack

$\left(C_{L_\alpha}\right)_t$ lift-curve slope of isolated tail

$C_{m_{i_t}}$ rate of change of pitching-moment coefficient with tail incidence angle

$\left(C_{m_{i_t}}\right)_o'$ value of $C_{m_{i_t}}$ at zero lift for high tail position with flaps neutral

l tail length, distance from $0.25\bar{c}$ to $0.25\bar{c}_t$, feet

z vertical distance, feet

Subscripts:

e effective

t tail

av average

o value at zero lift of the wing

MODEL AND APPARATUS

The wing plan form and some of the pertinent dimensions of the wing are given in figure 1. The wing had an aspect ratio of 2.84, a taper ratio of 0.616, and symmetrical circular-arc airfoil sections perpendicular to the maximum thickness line. A straight line connecting the

leading edge of the root and theoretical tip chord was swept back 52.05°. The maximum thickness of the airfoil sections parallel to the plane of symmetry was 6.5 percent chord at the root and 4.1 percent chord at the tip. The wing had neither geometric twist nor dihedral.

The wing was combined at zero incidence in a midposition with a fuselage of circular cross section (fig. 1). The fuselage had a fineness ratio of 10.2 and a maximum diameter of 34.6 percent of the wing-root chord. The ordinates of the fuselage are given in reference 2. Fillets were not employed at the juncture of the wing and fuselage.

The model was tested with round-nose, extensible, leading-edge flaps which had a constant chord of 3.80 inches and extended inboard from 0.975b/2 to 0.725b/2 (fig. 2). These flaps were deflected 37° from the wing-chord plane in a plane perpendicular to a line joining the leading edges of the root and tips chords.

Two types of trailing-edge flaps were used: One set located at the 80-percent-chord line are referred to as "split flaps" and the other set located at the 100-percent-chord line are referred to as "extended trailing-edge flaps." Both types of trailing-edge flaps were 20 percent of the wing chord and were deflected 60°, as shown in figure 2. The split flaps and extended trailing-edge flaps extended outward approximately 25 and 35 percent of the wing span, respectively, from the juncture of the wing and fuselage.

The horizontal tail had 42.05° sweepback at the leading edge, an aspect ratio of 4.01, a taper ratio of 0.625, and NACA 0012-64 airfoil sections parallel to the plane of symmetry. The mounting arrangement of the tail allowed the tail to be secured at various vertical positions. The tail positions 0.442b/2 above, 0.136b/2 above, and 0.132b/2 below the wing-chord plane (fig. 1) are referred to, respectively, as high, intermediate, and low. The vertical position of the tail is defined as the perpendicular distance from the wing-chord plane to the quarter-chord point of the mean aerodynamic chord of the tail. The incidence of the tail was measured with reference to the wing-chord plane and was changed by rotating it about the quarter-chord point of the mean aerodynamic chord of the tail. The accuracy of the measurement of the tail incidence angle is believed to be within ±0.2°.

The air-stream survey rake of the Langley 19-foot pressure tunnel was employed to obtain sidewash, downwash, and dynamic pressure. The rake is composed of six pitot-static tubes incorporating pitch and yaw orifices which were previously calibrated through a pitch range of ±18° and a yaw range of ±12°. A description of the rake is given in reference 3.

TESTS

Tests were made in the Langley 19-foot pressure tunnel with the model mounted on the two-support system. All tests were made at a tunnel air pressure of approximately 33 pounds per square inch, absolute. The Reynolds number (based on the M.A.C. of the wing) was 5.5×10^6 and the Mach number was approximately 0.11.

Measurements of lift, drag, and pitching moment were made through a range of angles of attack from -4° to 32° and air-flow surveys were made at angles of attack of approximately 3°, 8°, 13°, 16°, and 19°. The air-flow surveys were made in a vertical plane normal to the tunnel center line and were $1.71\bar{c}$ behind the quarter-chord point of the wing at 0° angle of attack. The plane of survey was selected as a compromise on the basis of the fore and aft variation with angle of attack of the quarter-chord point of the mean aerodynamic chord of the tail at various vertical positions. The maximum deviation of the tail quarter-chord point from the plane of survey occurred at high angles of attack. At the highest angle of attack (19°) the plane of survey corresponded to a tail length of $1.57\bar{c}$ for the high tail and a tail length of $1.87\bar{c}$ for the low tail.

REDUCTION OF DATA

Longitudinal characteristics.- The force and moment data presented have been reduced to nondimensional coefficient form and have been corrected for the support tare and strut interference. A correction for air-stream misalinement has been applied to the values of angle of attack and drag coefficient. Jet-boundary corrections to the angle of attack, drag coefficient, and pitching-moment coefficient were determined from reference 4 and are as follows:

$$\Delta\alpha = 0.94C_L$$

$$\Delta C_D = 0.0139C_L^2$$

For configurations with horizontal tail off

$$\Delta C_m = 0.0024C_L$$

and for configurations with the horizontal tail on

$$\Delta C_m = 0.0066 C_L$$

All corrections were added.

Effective downwash and dynamic pressure.- The values of effective downwash and dynamic-pressure ratio were determined from the pitching-moment data. A test of this tail (reference 5) indicated a constant lift-curve slope throughout the angle-of-attack range; hence, the method of determining ϵ_e and $(q_t/q)_e$ was simplified to

$$\epsilon_e = \alpha + i_t - \alpha_t$$

where

$$\alpha_t = \frac{C_{m_t}}{C_{m_{i_t}}}$$

and

$$\left(\frac{q_t}{q}\right)_e = \frac{C_{m_{i_t}}}{\left(C_{m_{i_t}}\right)_o}$$

The effective values of downwash and dynamic-pressure ratio for the low tail were not computed above an angle of attack of 20° because the reliability of the pitching-moment data for this particular angle-of-attack range and tail configuration are considered doubtful.

Horizontal tail efficiency.- The tail efficiency factor is based on a value of $\left(C_{m_{i_t}}\right)_o'$ obtained in the region of zero lift with flaps neutral and with the tail in the high position. For this condition it is assumed that the wing-fuselage combination has a negligible effect on the flow over the tail. The tail efficiency factor η was obtained as follows:

$$\eta = \frac{\left(C_{m_{i_t}}\right)_o}{\left(C_{m_{i_t}}\right)_o'}$$

Tail stability parameter.- The combined effects of downwash angle and dynamic pressure on the stabilizing contribution of the horizontal

tail is defined by the tail stability parameter τ. The derivation of τ is as follows:

$$C_{m_t} = -\left(C_{L_\alpha}\right)_t \alpha_t \left(\frac{q_t}{q}\right)_e T\eta \tag{1}$$

differentiating with respect to α

$$\frac{dC_{m_t}}{d\alpha} = -\left(C_{L_\alpha}\right)_t T\eta \left[\left(\frac{q_t}{q}\right)_e \frac{\partial \alpha_t}{\partial \alpha} + \alpha_t \frac{\partial \left(\frac{q_t}{q}\right)_e}{\partial \alpha}\right] \tag{2}$$

where

$$\frac{\partial \alpha_t}{\partial \alpha} = \frac{\partial(\alpha - \epsilon_e + i_t)}{\partial \alpha} = 1 - \frac{\partial \epsilon_e}{\partial \alpha} \tag{3}$$

$$\frac{dC_{m_t}}{d\alpha} = -\left(C_{L_\alpha}\right)_t T\eta \left[\left(\frac{q_t}{q}\right)_e \left(1 - \frac{\partial \epsilon_e}{\partial \alpha}\right) + \alpha_t \frac{\partial \left(\frac{q_t}{q}\right)_e}{\partial \alpha}\right] \tag{4}$$

Then, grouping the terms containing the flow parameters ϵ and $\frac{q_t}{q}$ gives

$$\frac{dC_{m_t}}{d\alpha} \frac{1}{\left(C_{L_\alpha}\right)_t T} = \tau = -\eta \left[\left(\frac{q_t}{q}\right)_e \left(1 - \frac{\partial \epsilon_e}{\partial \alpha}\right) + \alpha_t \frac{\partial \left(\frac{q_t}{q}\right)_e}{\partial \alpha}\right] \tag{5}$$

The values presented were obtained using the relationship

$$\tau = \frac{dC_{m_t}}{d\alpha} \frac{1}{\left(C_{L_\alpha}\right)_t T}$$

where

$\left(C_{L_\alpha}\right)_t = 0.0495$ (determined from isolated tail data, reference 5)

and

$T = 0.2805$ (determined from geometry of model)

When the tail is contributing stability, the sign of τ is negative.

The values of τ presented herein were obtained with a fixed tail incidence, and in some cases large out-of-trim conditions resulted. It may be seen from equation (5) however, that, when $\frac{\partial\left(\frac{q_t}{q}\right)_e}{\partial\alpha}$ is zero, the values of τ are independent of the tail load. Hence, these values of τ are applicable to any degree of trim or to any center-of-gravity location. Through the angle-of-attack range for which the tail passes through the wake, finite values of $\frac{\partial\left(\frac{q_t}{q}\right)_e}{\partial\alpha}$ are obtained; therefore, the values of τ through that angle-of-attack range are more nearly applicable to the center-of-gravity location at which the measured tail load would provide trim when the tail is at the wake center.

It has been found that, through the angle-of-attack range for which $\frac{\partial\left(\frac{q_t}{q}\right)_e}{\partial\alpha}$ of the present investigation is maximum, values of τ are applicable to a trim condition for a center-of-gravity location rearward of the quarter-chord point of the mean aerodynamic chord. An analysis was made to determine the effects of trim on the values of τ with the center of gravity located at the quarter-chord point of the mean aerodynamic chord. It was found that, when values of $\frac{\partial\left(\frac{q_t}{q}\right)_e}{\partial\alpha}$ were significant, the changes in α_t required to provide trim were such that the product of these terms produced only minor effects on the trends indicated by the variations of τ presented.

The values of τ for the low tail are presented for nearly the entire angle-of-attack range; however, those values of τ at angles of attack greater than approximately 20° need qualifying. It was not possible to determine accurately $\frac{dC_{m_t}}{d\alpha}$ in the range above an angle of attack of approximately 20°; hence, the absolute values of τ given for that range are open to question. It is believed, however, that the values presented reliably indicate the trends that exist.

Local air-flow characteristics.- The air-stream survey data have been corrected for jet-boundary effects by an angle change to the downwash and a downward displacement of the flow field relative to the wing-chord plane.

Some air-flow conditions were encountered which exceeded the limits of the survey-rake calibration. Data for these conditions were obtained from a linear extrapolation of the rake calibration. The inaccuracies introduced by extrapolating are believed to be relatively small for values of downwash angle less than 27°.

The fact that the dynamic pressures measured outside of the wake at the highest angles of attack slightly exceeded unity may be attributed to the wake blockage in the closed tunnel. No corrections have been made for this blockage.

Average values of dynamic pressure and downwash.- For purpose of evaluating air-flow surveys at a particular vertical position, average weighted values of dynamic-pressure ratio and downwash were determined for tail positions corresponding to those considered in the tail-on tests. The following equations define the manner in which these values were obtained:

$$\left(\frac{q_t}{q}\right)_{av} = \frac{2}{S_t}\int_0^{b_t/2} \left(\frac{q_t}{q}\right) c_t \, dy$$

$$\epsilon_{av} = \frac{2}{S_t\left(\frac{q_t}{q}\right)_{av}}\int_0^{b_t/2} \left(\frac{q_t}{q}\right) \epsilon c_t \, dy$$

RESULTS AND DISCUSSION

Presentation of Results

The longitudinal characteristics of the wing and fuselage are presented in figures 3 to 5. The results of tests of several wing configurations with a horizontal tail located at various vertical positions are presented in figures 6 to 8. A summary of the longitudinal stability characteristics of the wing with and without the horizontal tail is given in table I. The results concerning the characteristics of the air flow behind the wing are presented in figures 9 to 12 and table II.

Effect of Fuselage on Longitudinal Characteristics of the Wing

The data presented in figure 3 show that the addition of a fuselage to the plain wing resulted in an increase in the value of maximum lift coefficient from 1.04 to 1.16. The fuselage caused only small changes in the pitching moment through the lift range of the plain wing. With the 0.25b/2 leading-edge-flap configuration (fig. 4), the maximum lift coefficient obtained with the fuselage on was 1.26 as compared to 1.06 with the fuselage off. With the fuselage on, as with the fuselage off, a rearward shift of the aerodynamic center occurred at a lift coefficient of approximately 0.9. This shift of the aerodynamic center was less with the fuselage on than with the fuselage off. An increase in the maximum lift coefficient of the configuration with 0.25b/2 leading-edge and 0.50b/2 extended trailing-edge flaps was realized with the addition of the fuselage; however, the increase in lift was accompanied by an unstable variation of the pitching-moment curve (fig. 5) above a lift coefficient of 1.35.

These changes in the longitudinal characteristics of the wing are believed to be associated with an outboard shift of the origin of the vortex flow (discussed in reference 1) from the apex of the wing to the juncture of the wing and fuselage in addition to a delay of the effects of the vortex flow on the rear parts of the inboard sections of the wing.

Effect of Tail Position on Stability and Tail Effectiveness

Longitudinal stability.- In general, the stability characteristics of the wing-fuselage configuration in combination with a horizontal tail were nonlinear through the angle-of-attack range (fig. 6). At low angles of attack an increase in the stability of the wing-fuselage combination was realized with the addition of the tail at either the high, low, or intermediate positions. The variations of dC_m/dC_L with angle of attack presented in figure 7 show that the increase in stability up to about 4° angle of attack was nearly the same for all tail positions investigated. The increase in stability realized with the tail located above the wing-chord plane decreased with an increase in angle of attack, so that at high angles of attack the high tail had a destabilizing effect with both the flap-off and the flap-deflected configurations. At moderate angles of attack of the flap-off configuration the changes in dC_m/dC_L (fig. 7), which are indicative of a forward shift of the center of pressure, decreased with decrease in tail height; however,

appreciable changes in dC_m/dC_L persisted through the moderate angle-of-attack range even with the low tail. The changes in dC_m/dC_L of the wing-fuselage combination were decreased up to approximately 16° angle of attack when the 0.25b/2 leading-edge flaps were deflected, thereby greatly reducing the changes in stability through the moderate angel-of-attack range of the configuration with either the low tail or intermediate tail. With the tail at either of these positions the value of dC_m/dC_L increased rapidly in the negative direction at angles of attack greater than approximately 16°. The abrupt increase in dC_m/dC_L for the intermediate tail and the low tail occurred at a much lower angle of attack with the trailing-edge flaps deflected.

Figure 6 shows that large out-of-trim conditions were encountered at moderate and high angles of attack, particularly with the intermediate and low tails. As previously indicated, the effects of trim on the stabilizing contribution of the tail were minor; therefore, the stability for a trim condition will not be appreciably different from that indicated in figure 7. With either of these tails the change of static margin through the lift range as indicated by curves of dC_m/dC_L (fig. 7) might be undesirable.

Tail effectiveness.- The values of τ presented in figure 6 show the stabilizing effect of the tail at various vertical positions. These results indicate that although the tail had a stabilizing effect at low angles of attack for all vertical positions tested, the high tail and, in most cases, the intermediate tail approached ineffectiveness ($\tau = 0$) in the moderate angle-of-attack range at approximately the same angle of attack. With further increase of angle of attack, the effect of the intermediate tail became progressively more stabilizing, whereas that of the high tail became destabilizing. This decrease in the effectiveness of the tail is the result of an increase in the value of $\partial\epsilon_e/\partial\alpha$ as indicated by the downwash curves in figure 6. At high angles of attack the difference in effectiveness of the high and intermediate tail is associated with the lower values of $\partial\epsilon_e/\partial\alpha$ for the intermediate tail. The low tail, in general, provided the most favorable stabilizing effect through moderate and high angles of attack.

The 0.25b/2 leading-edge flaps improved the effectiveness of the intermediate tail so that the resulting stability was comparable with that obtained with the low tail. The effectivness of the low and high tails, however, was not appreciably altered by leading-edge flaps.

The effects of trailing-edge flaps on effectiveness of the tail may be seen by comparing the variations of τ with angle of attack presented in figure 6(b) with figure 6(c) and figure 6(d). Although

the trailing-edge flaps caused some significant changes in effectiveness of the tail, no appreciable change in the stability of the 0.25b/2 leading-edge-flap configuration was realized.

In order to indicate the effect of wing airfoil section on the tail, the effectiveness of the tail presented herein was compared with that realized with an NACA 64-series wing (reference 6) having a plan form nearly identical to that of the present wing (fig. 8). For a given vertical position of the tail the variation of τ with lift coefficient of the circular-arc wing was, in general, similar to those with the NACA 64-series wing. The existing differences are believed associated mainly with the vortex flow which formed at a much lower lift coefficient with the circular-arc wing than with the NACA 64-series wing.

Air-Flow Characteristics

The air-flow survey data have been cross plotted to obtain contour charts of dynamic-pressure ratio, downwash, and sidewash. The charts are presented in figures 9 and 10. In order to determine the applicability of the survey data for design purposes, pitching-moment characteristics were calculated using average values of downwash and dynamic-pressure ratio listed in table II. A comparison of the pitching-moment characteristics obtained by calculation and by experiment is shown in figure 11. The main difference appears as a trim change and may be accounted for by (1) the fact that measurement in the single survey plane may not be accurately representative of the flow over the swept tail surface and (2) the fact that some of the survey data were obtained from an extrapolation of the survey-rake calibration. In general, the agreement of the calculated and measured longitudinal stability characteristics indicates that the contribution of the horizontal tail to the longitudinal stability of the wing can be predicted with a fair degree of accuracy by use of air-flow characteristics.

Figures 9 and 10 show that regions of large downwash were encountered above the wake center. By considering the tail positions used in this investigation, it may be seen from the contours of dynamic-pressure ratio of the flap-off configuration (fig. 9) that both the high and intermediate tail positions were above or at the center of the wake for the angle-of-attack range up to 16.2°. The low tail position, however, was below the wake center for the moderate and high angles of attack. Although the wake was displaced downward for the flap-deflected configuration (fig. 10), this displacement was such that the position of the various tails relative to the wake center was not appreciably different from that found in the case of the flap-off configuration.

A plot of local downwash angle with angle of attack is presented in figure 12 for several spanwise stations of a tail at positions

previously considered. These results indicate that, at moderate angles of attack, $\partial\epsilon/\partial\alpha$ increased to an undesirably high value for both the high and intermediate tail positions. These increases in $\partial\epsilon/\partial\alpha$ resulted in a decrease of the effectiveness of the tail in the positions above the wing-chord plane and a decrease in the stability at moderate angles of attack. Beyond an angle of attack of approximately 16° the intermediate tail appears to be in a flow where the rate of change of downwash angle with angle of attack had a favorable influence on the stability contributed by the tail. The low tail in combination with the flap-off configuration appears to be influenced by a highly favorable rate of change of downwash angle with angle of attack. With the flaps deflected, an undesirable increase in $\partial\epsilon/\partial\alpha$ occurred at a station corresponding to $0.90b_t/2$ of the low tail; however, a highly favorable negative rate of change of downwash angle with angle of attack existed at a station corresponding to $0.70b_t/2$, which appears very influential on the over-all effect of the tail (fig. 6(d)).

A comparison of the characteristics of the air flow behind the present wing with those obtained with a similar plan form but incorporating NACA 64-series airfoil sections (reference 6) indicates that the characteristics of the flow are similar. Although regions of high downwash and sidewash angles are exhibited above the wing-chord plane of both wings at high angles of attack, the magnitude of these angles at a given angle of attack is noticeably greater for the circular-arc wing than for the round-nose wing. This difference is the result of greater lift developed at a given angle of attack by the circular-arc wing than by the round-nose wing.

CONCLUDING REMARKS

The results of tests to determine the effects of a horizontal tail and fuselage on the low-speed longitudinal characteristics of a circular-arc 52° sweptback wing indicate that:

The low tail (located 0.132 semispan below the wing-chord plane) was situated below the wake center for moderate and high angles of attack and had a stabilizing influence through the angle-of-attack range because of a favorable rate of change of downwash angle with angle of attack. The intermediate and high tails (located 0.136 and 0.442 semispan above the wing-chord plane) had a stabilizing influence at low angles of attack; however, at moderate and high angles of attack large increases in the rate of change of downwash with angle of attack

cause a decrease in the stabilizing effect of these tails. The effect of the high tail actually became destabilizing at high angles of attack.

The most favorable improvements in dC_m/dC_L (rate of change of pitching-moment coefficient with lift coefficient) were obtained with the low and intermediate tails. Although all configurations with these tails were considerably out of trim at high angles of attack, an analysis indicated that the effects of trim would not appreciably change the stability realized with these tails. With either of these tails the change in static margin through the lift range might be undesirable.

The 0.25 semispan leading-edge flaps increased the maximum lift coefficient, improved the stability of the wing-fuselage configuration in the high angle-of-attack range, and reduced the changes in dC_m/dC_L realized through the moderate angle-of-attack range with either the intermediate tail or low tail.

The addition of a fuselage to the wing resulted in an increase in maximum lift coefficient. With the fuselage on, some improvement was realized in the variation of dC_m/dC_L in the high angle-of-attack range of the 0.25-semispan leading-edge-flap configuration; however, in general, the effects of the fuselage on the stability of the wing were small.

The stabilizing contribution of the horizontal tail can be predicted with a fair degree of accuracy from the air-flow survey data.

Langley Aeronautical Laboratory
National Advisory Committee for Aeronautics
Langley Field, Va.

REFERENCES

1. Foster, Gerald V., and Griner, Roland F.: Low-Speed Longitudinal Characteristics of a Circular-Arc 52° Sweptback Wing of Aspect Ratio 2.84 with and without Leading-Edge and Trailing-Edge Flaps at Reynolds Numbers from 1.6×10^6 to 9.7×10^6. NACA RM L50F16a, 1950.

2. Woods, Robert L., and Spooner, Stanley H.: Effects of High-Lift and Stall-Control Devices, Fuselage, and Horizontal Tail on a Wing Swept Back 42° at the Leading Edge and Having Symmetrical Circular-Arc Airfoil Sections at a Reynolds Number of 6.9×10^6. NACA RM L9B11, 1949.

3. Salmi, Reino J.: Horizontal-Tail Effectiveness and Downwash Surveys For Two 47.7° Sweptback Wing-Fuselage Combinations with Aspect Ratios of 5.1 and 6.0 at a Reynolds Number of 6.0×10^6. NACA RM L50K06, 1951.

4. Eisenstadt, Bertram J.: Boundary-Induced Upwash for Yawed and Swept-Back Wings in Closed Circular Wind Tunnels. NACA TN 1265, 1947.

5. Spooner, Stanley H., and Martina, Albert P.: Longitudinal Stability Characteristics of a 42° Sweptback Wing and Tail Combination at a Reynolds Number of 6.8×10^6. NACA RM L8E12, 1948.

6. Griner, Roland F., and Foster, Gerald V.: Low-Speed Longitudinal and Wake Air-Flow Characteristics at a Reynolds Number of 6.0×10^6 of a 52° Sweptback Wing Equipped with Various Spans of Leading-Edge and Trailing-Edge Flaps, a Fuselage, and a Horizontal Tail at Various Vertical Positions. NACA RM L50K29, 1950.

Table I.- Summary of longitudinal stability characteristics of a 52° sweptback wing in combination with a fuselage and horizontal tail.

Wing configuration / Tail position (percent b/2)	Flaps off	0.25b/2 leading-edge flaps	0.25b/2 leading-edge flaps and 0.50b/2 extended trailing-edge flaps	0.25b/2 leading-edge flaps and 0.40 b/2 split flaps
Tail off	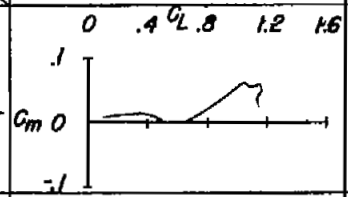	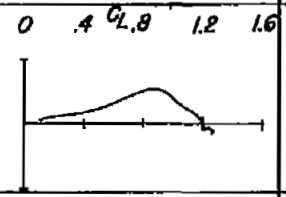	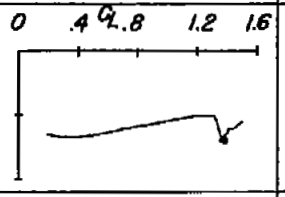	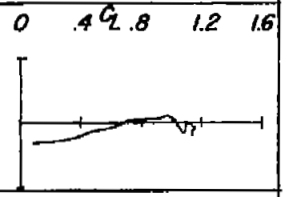
44.2	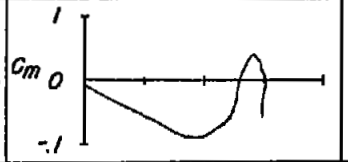	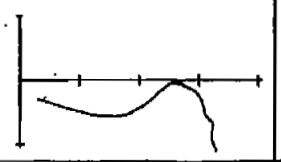	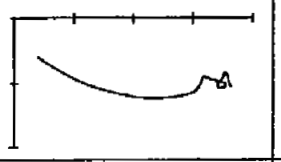	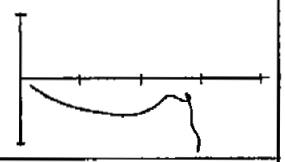
13.6	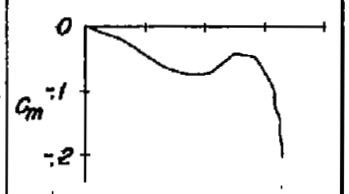	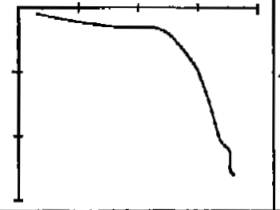	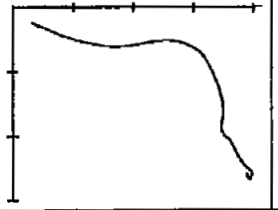	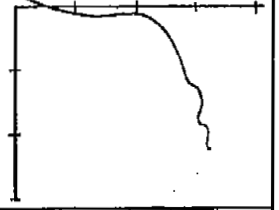
- 13.2	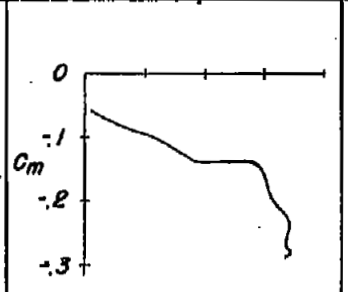	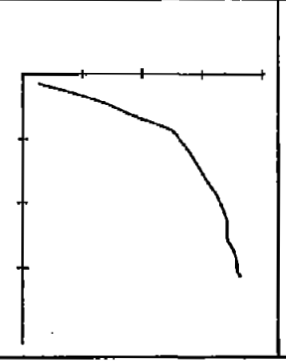	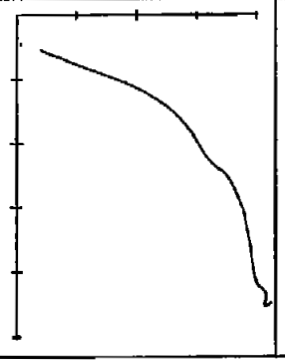	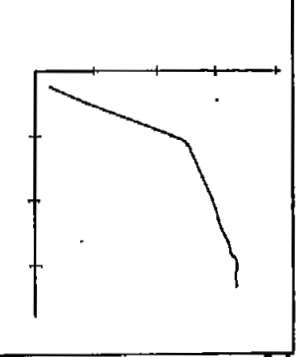

NACA

TABLE II.- EFFECTIVE AND AVERAGE VALUES OF DYNAMIC-PRESSURE RATIO AND DOWNWASH ANGLE AT THE TAIL OF A 52° SWEPTBACK WING-FUSELAGE COMBINATION WITH AND WITHOUT LEADING-EDGE AND TRAILING-EDGE FLAPS

Wing configuration	Tail position (percent b/2)	α (deg)	$\left(\frac{q_t}{q}\right)_e$ (a)	$\left(\frac{q_t}{q}\right)_{av}$ (b)	ϵ_e (deg) (a)	ϵ_{av} (deg) (b)	η
Flaps off	44.2	3.2	1.00	1.01	3.3	2.3	1.00
		8.1	.98	1.01	5.7	5.3	
		13.1	1.02	1.02	9.2	9.3	
		16.2	1.00	1.02	12.9	13.1	
		19.0	1.00	1.04	17.3	17.5	
	13.6	3.2	1.00	0.97	4.2	3.1	0.97
		8.1	1.00	.94	6.7	6.5	
		13.1	1.00	.94	10.1	10.2	
		16.2	1.00	.91	12.9	13.3	
		19.0	1.00	.86	15.2	15.2	
	-13.2	3.2	1.00	0.93	-0.8	0.3	0.925
		8.1	1.00	.91	1.3	2.5	
		13.1	.95	.98	3.3	5.0	
		16.2	.98	.97	4.8	6.3	
		19.0	.96	.97	6.3	7.6	
0.25b/2 leading-edge flaps and 0.40b/2 split flaps	44.2	3.4	1.00	1.02	5.1	4.2	1.00
		8.3	1.00	1.03	7.6	7.1	
		13.1	.91	1.03	11.8	11.4	
		16.3	.87	1.04	15.6	15.1	
		19.0	.86	.94	19.3	20.3	
	13.6	3.4	0.98	0.98	8.3	6.9	1.00
		8.3	.97	.98	11.4	10.5	
		13.1	.92	.89	15.6	16.2	
		16.3	.84	.84	17.2	17.5	
		19.0	.77	.80	17.3	15.2	
	-13.2	3.4	0.98	0.80	3.2	4.4	0.85
		8.3	1.02	.86	4.6	6.7	
		13.1	1.00	.87	5.0	7.1	
		16.3	.98	.91	4.6	5.6	
		19.0	.99	.99	5.0	7.4	

[a]Effective values (e) calculated from force-test data.
[b]Average values (av) calculated from air-flow survey data.

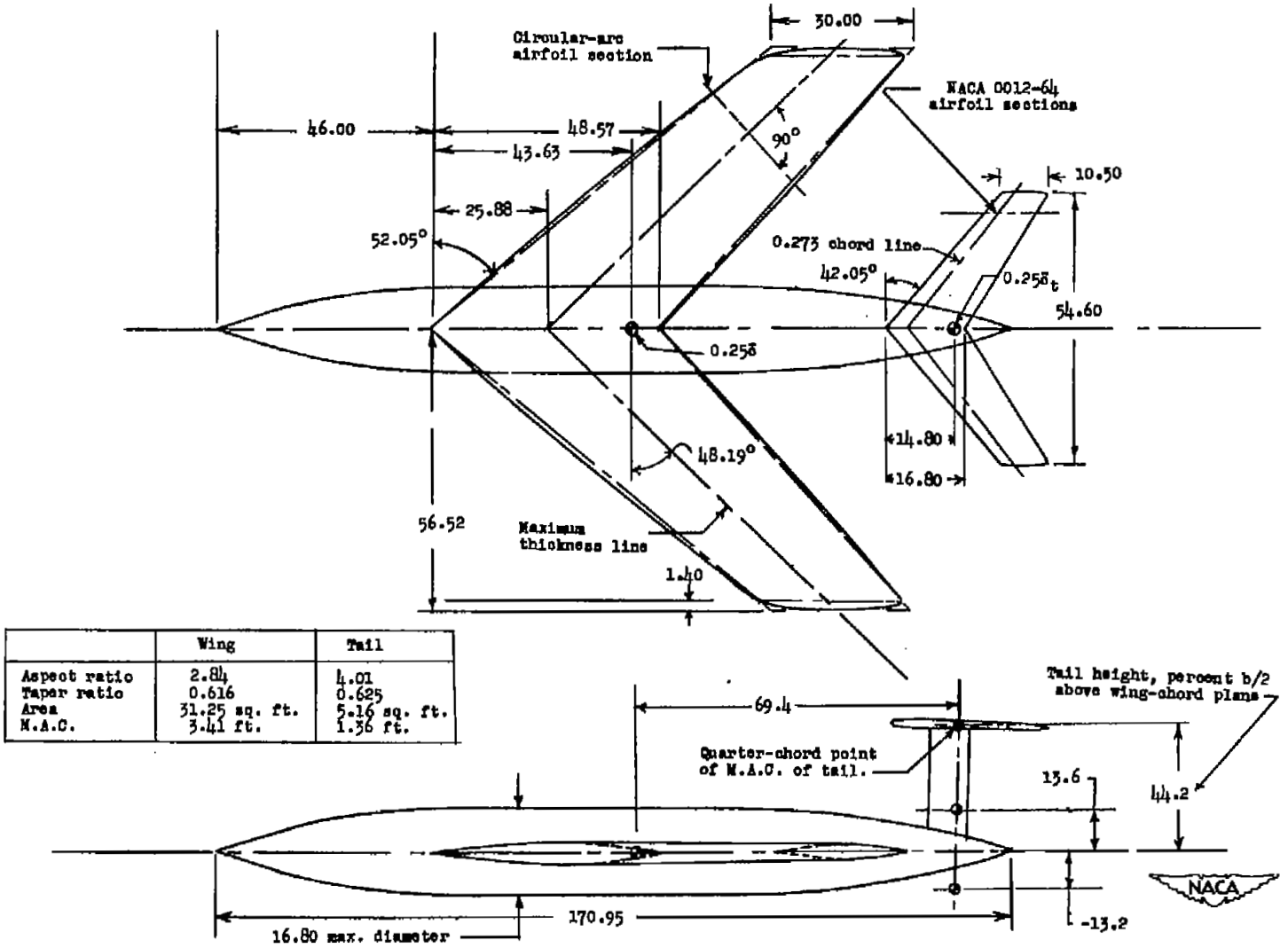

	Wing	Tail
Aspect ratio	2.84	4.01
Taper ratio	0.616	0.625
Area	31.25 sq. ft.	5.16 sq. ft.
M.A.C.	3.41 ft.	1.36 ft.

Figure 1.- Geometry of wing, fuselage, and horizontal tail. All dimensions are in inches unless otherwise noted.

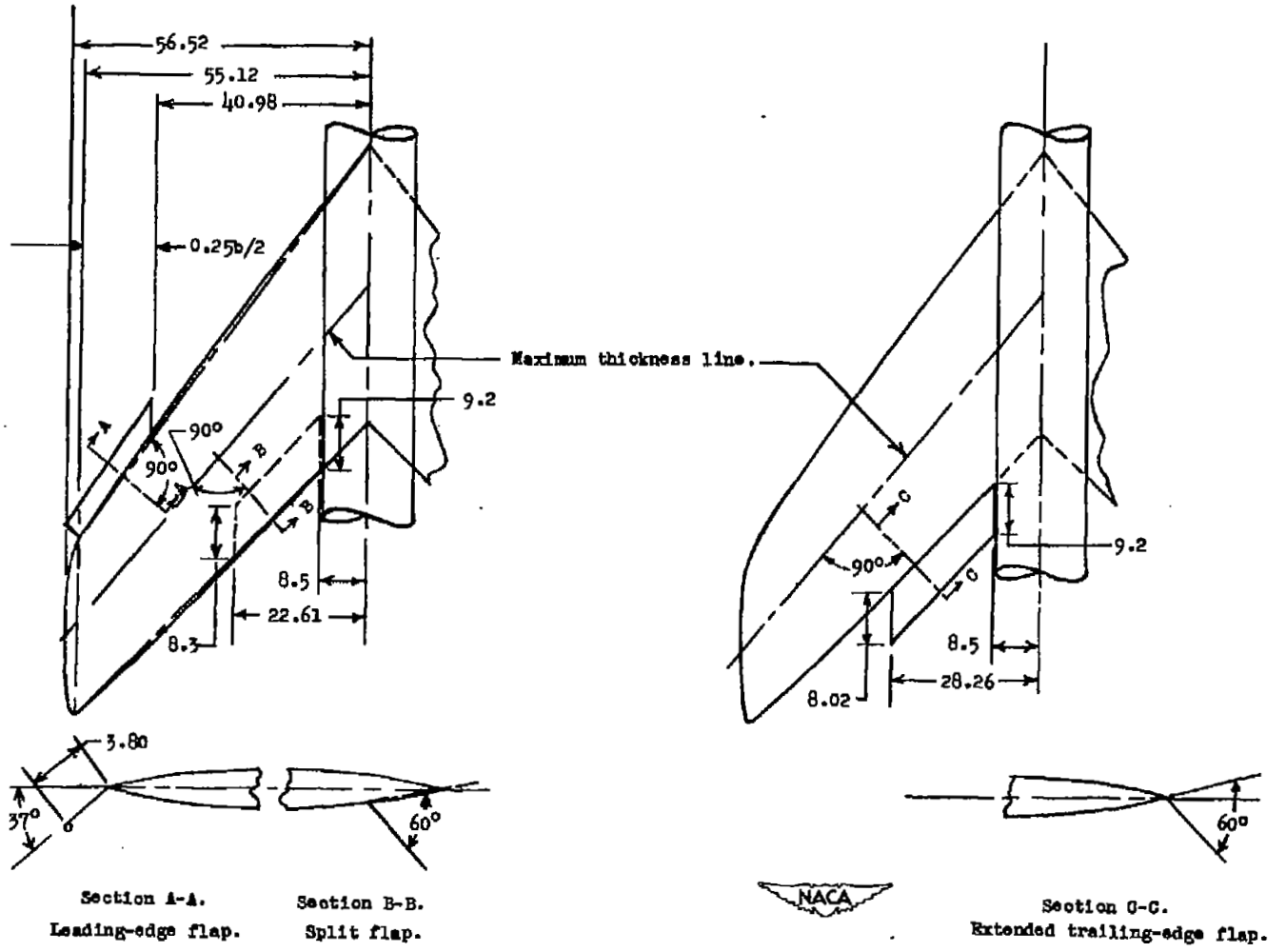

Figure 2.- Details of leading-edge and trailing-edge flaps on a 52° sweptback wing. All dimensions are given in inches unless otherwise noted.

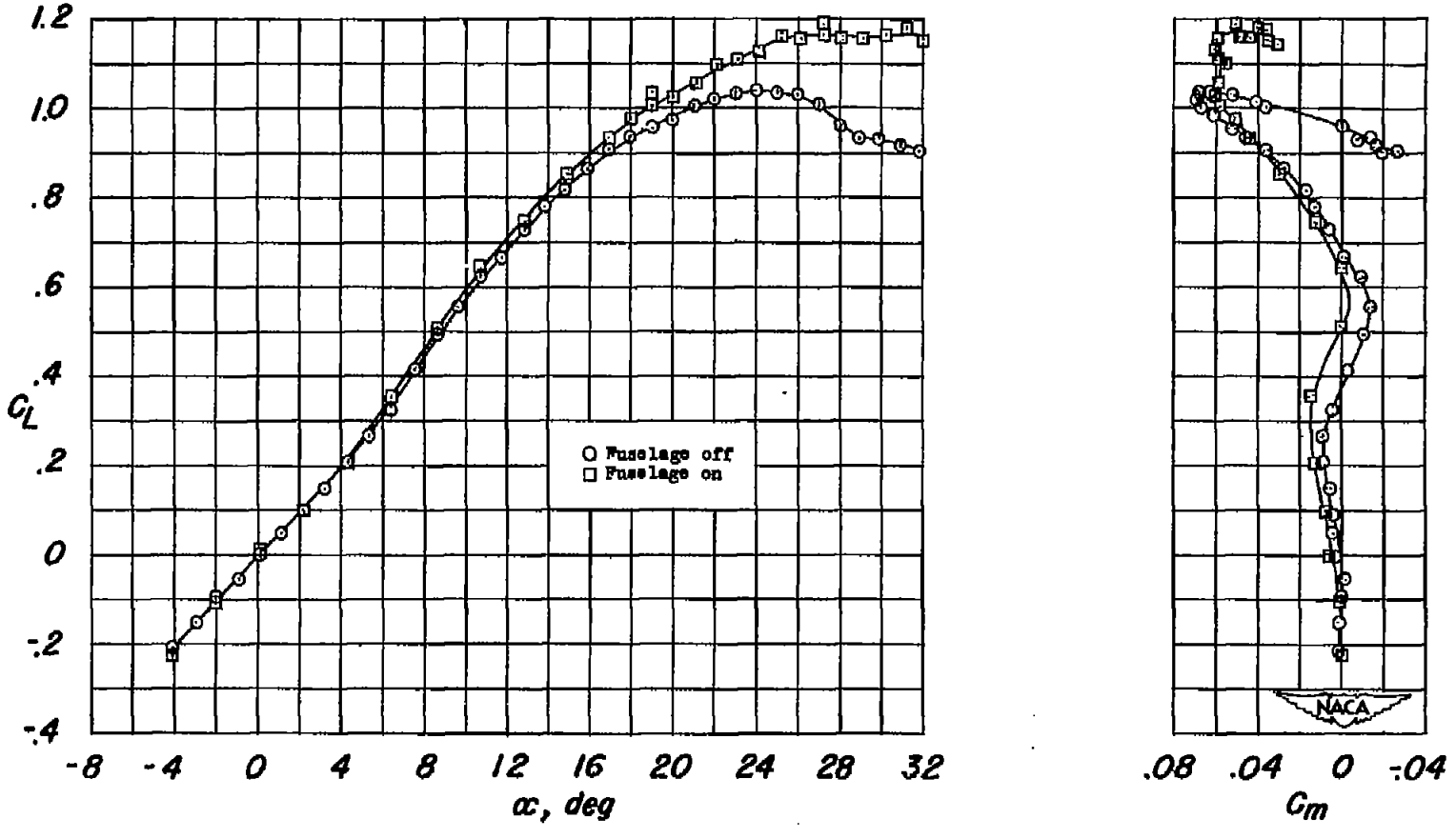

(a) C_L plotted against α and C_m.

Figure 3.- Effect of a fuselage on the aerodynamic characteristics of a 52° sweptback wing. $R = 5.5 \times 10^6$.

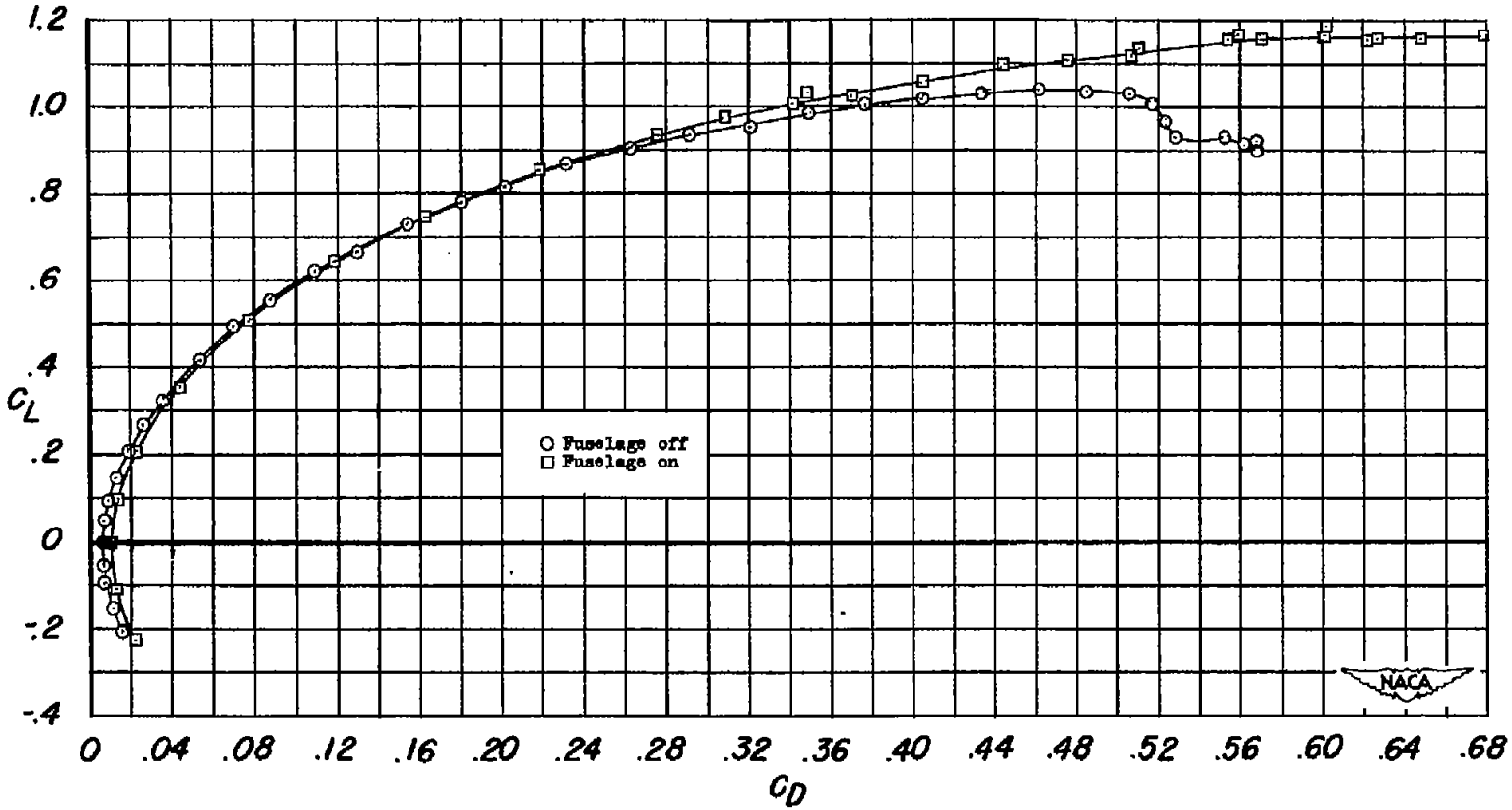

(b) C_L plotted against C_D.

Figure 3.- Concluded.

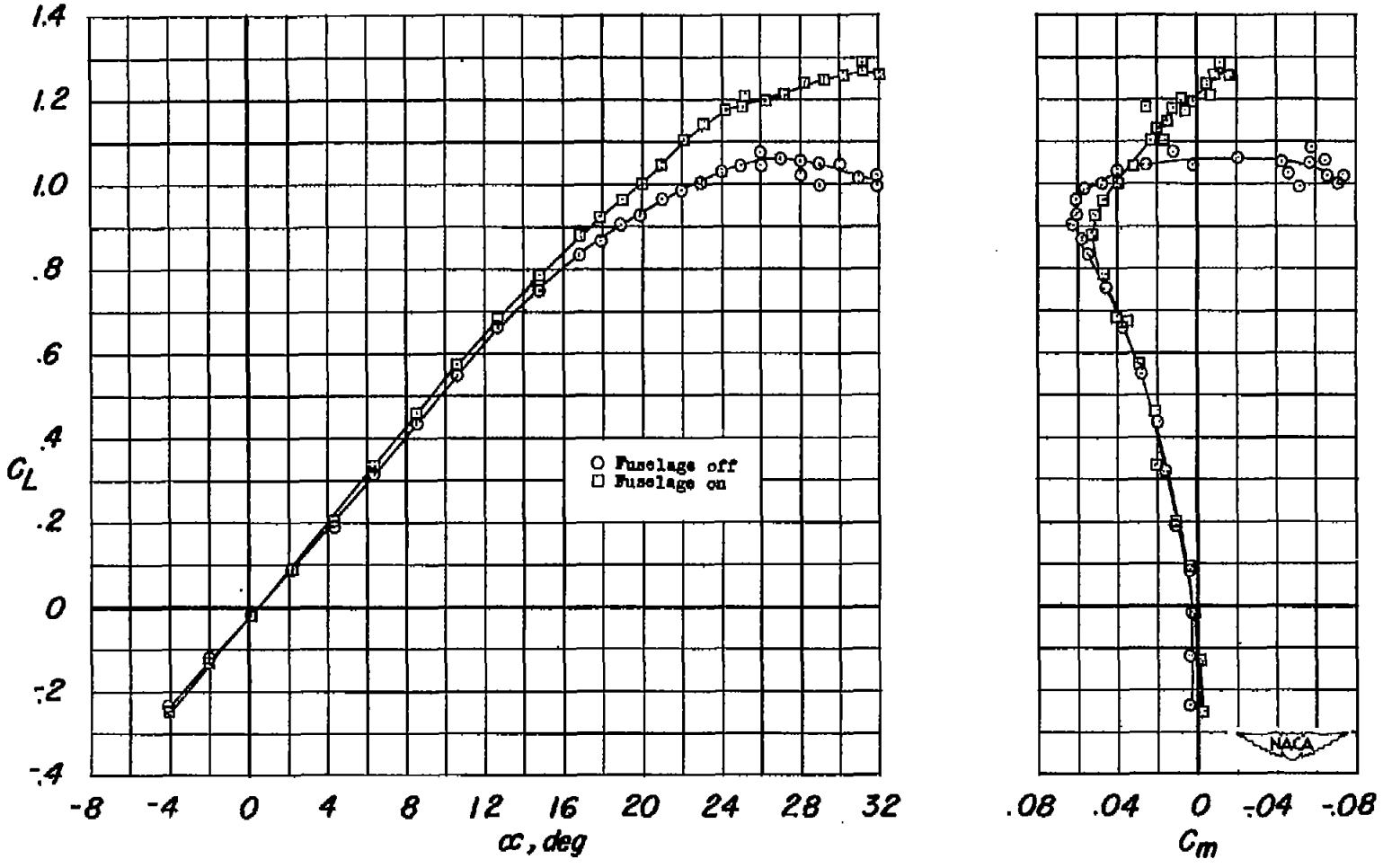

(a) C_L plotted against α and C_m.

Figure 4.- Effect of a fuselage on the aerodynamic characteristics of a 52° sweptback wing with 0.25b/2 extensible leading-edge flaps. $R = 5.5 \times 10^6$.

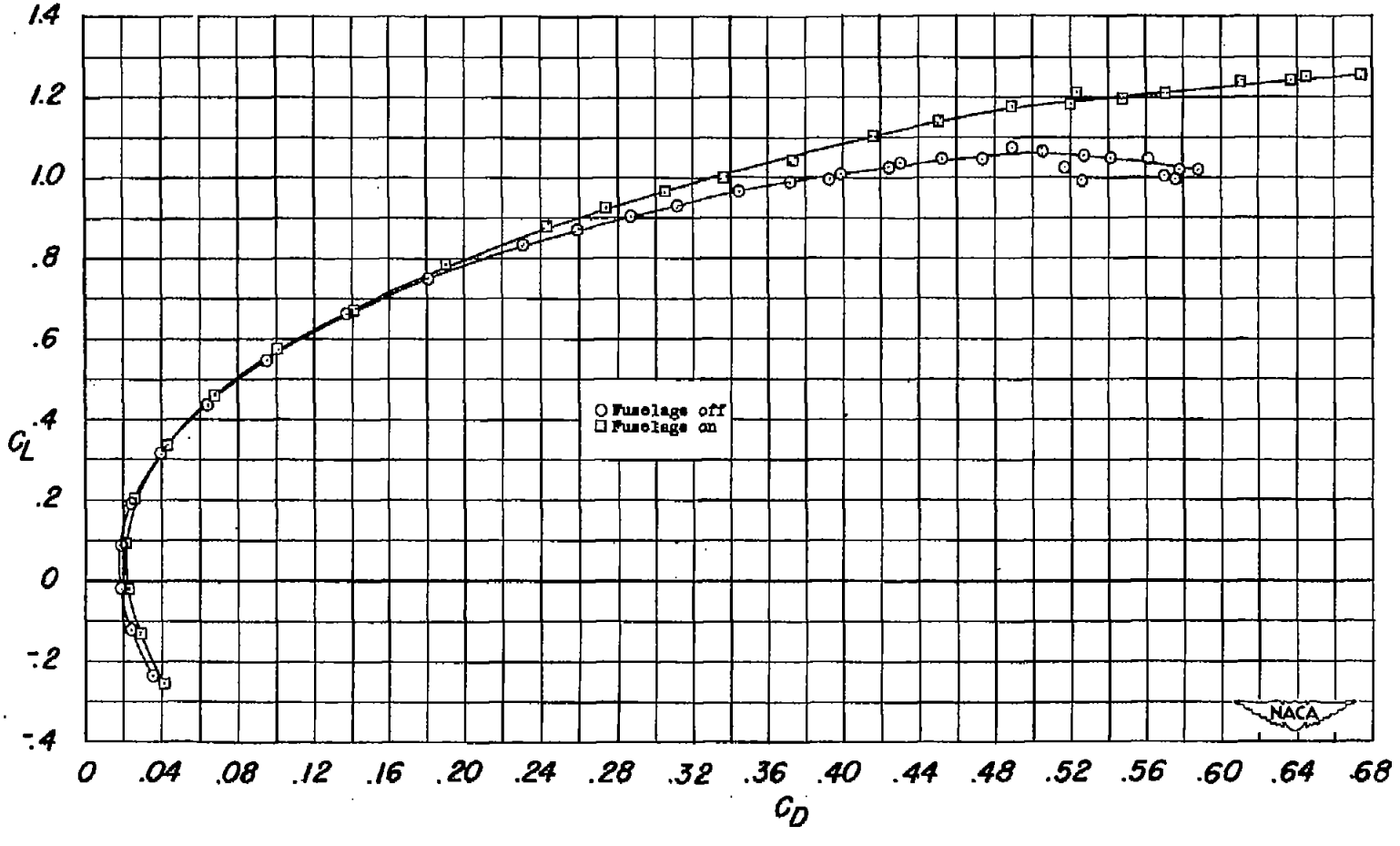

(b) C_L plotted against C_D.

Figure 4.- Concluded.

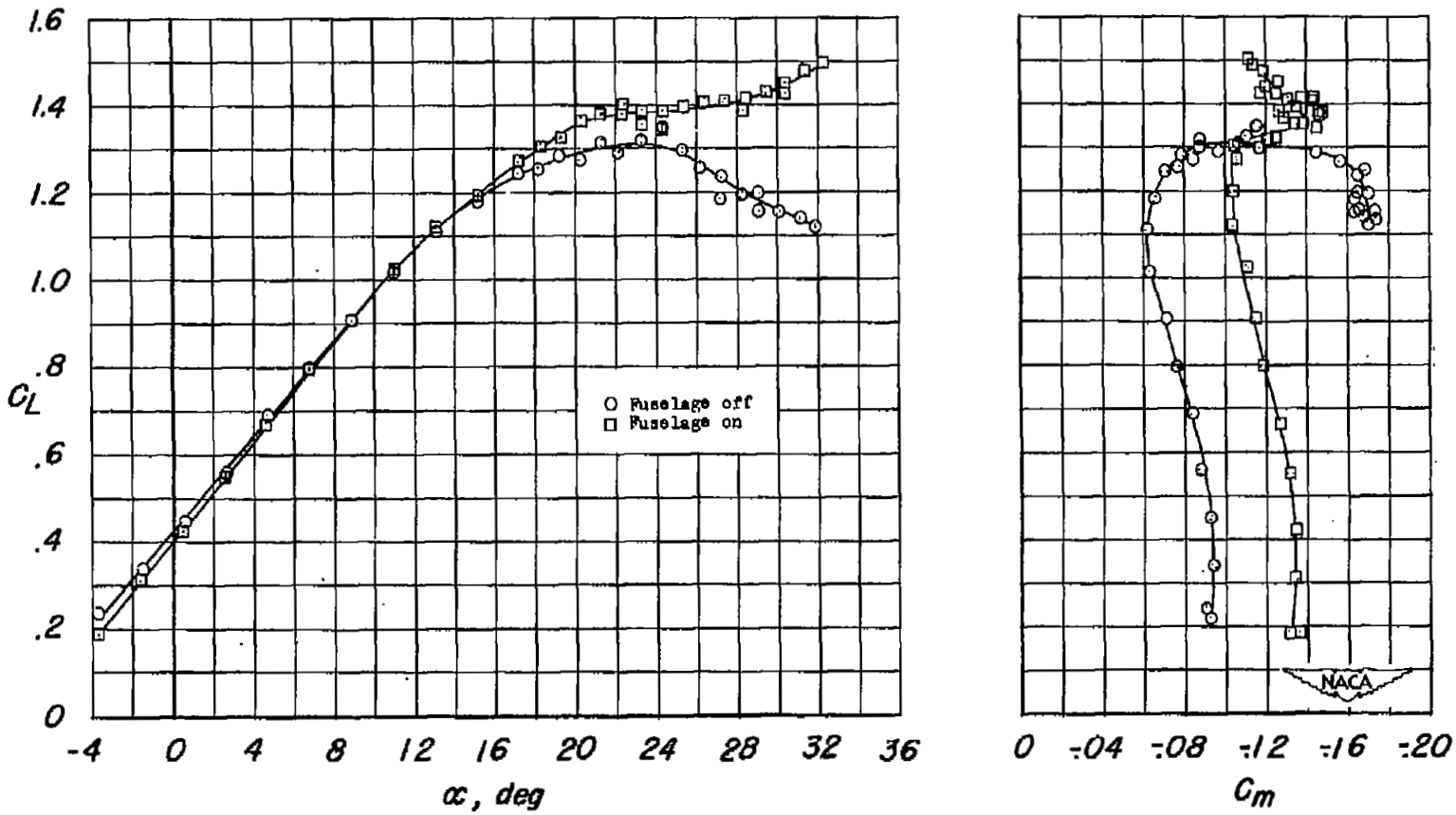

(a) C_L plotted against α and C_m.

Figure 5.- Effect of a fuselage on the aerodynamic characteristics of a 52° sweptback wing with 0.25b/2 extensible leading-edge flaps and 0.50b/2 extended trailing-edge flaps. $R = 5.5 \times 10^6$.

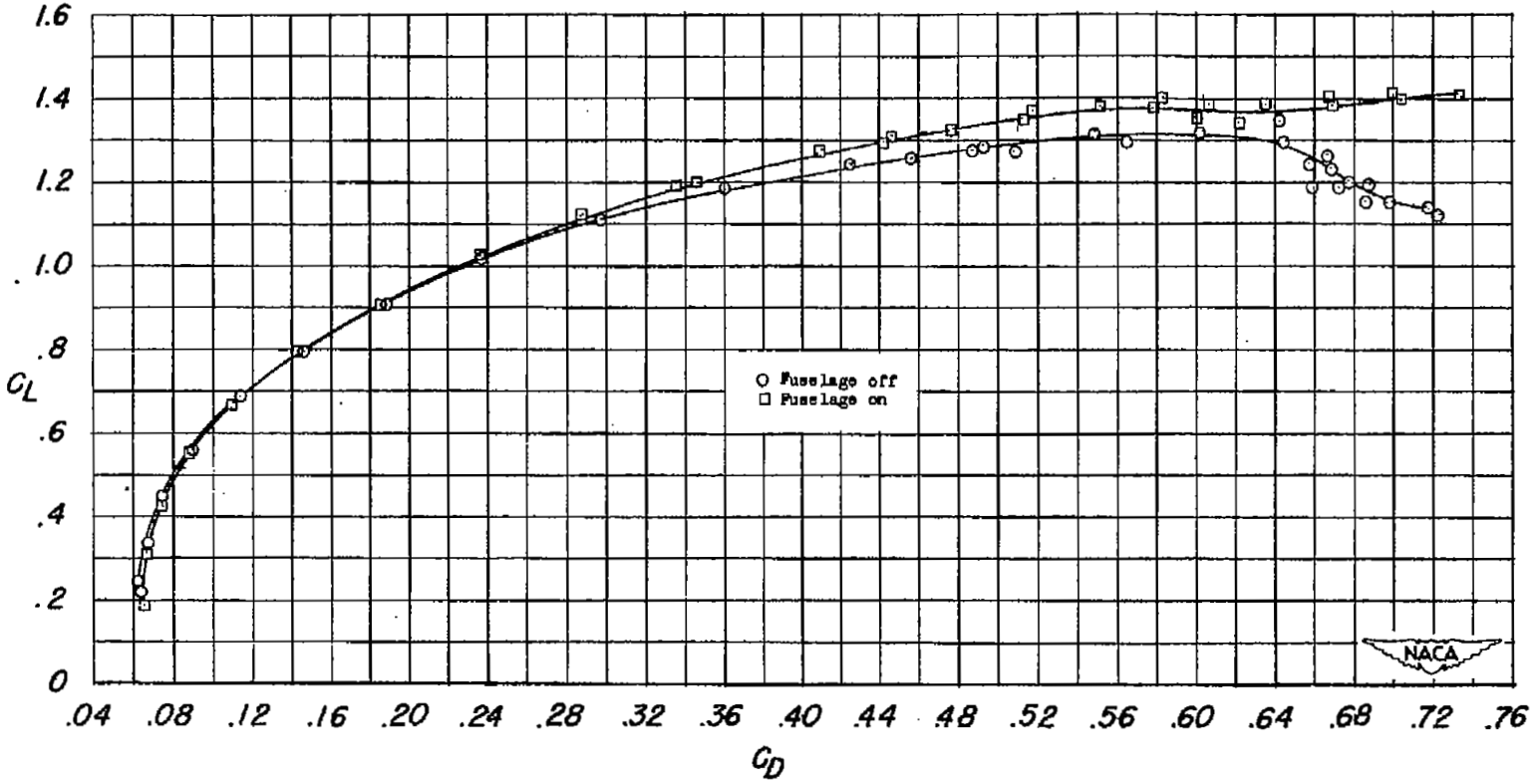

(b) C_L plotted against C_D.

Figure 5.- Concluded.

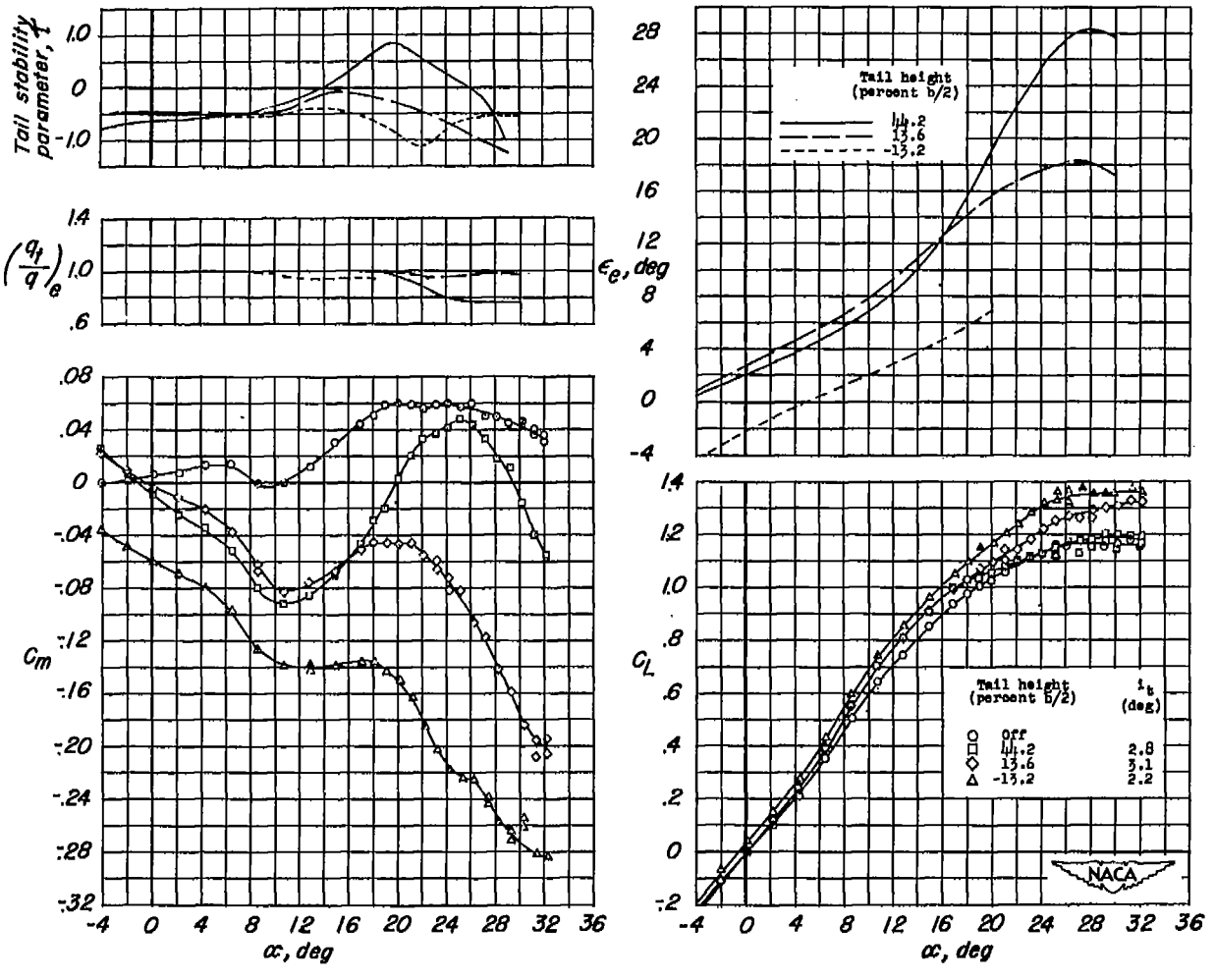

(a) Wing configuration - plain wing.

Figure 6.- Longitudinal characteristics of a 52° sweptback wing-fuselage combination with horizontal tail. Flaps off; $R = 5.5 \times 10^6$.

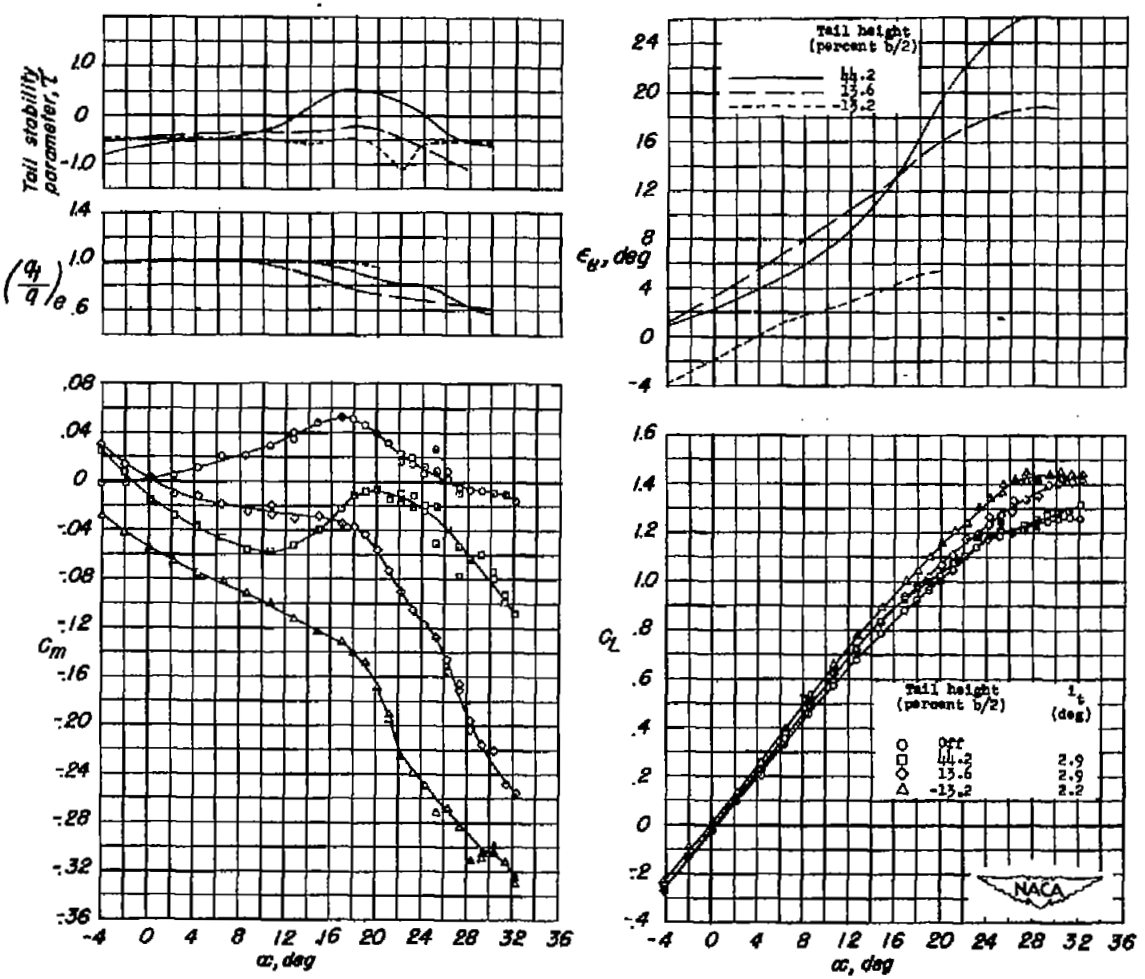

(b) Wing configuration, 0.25b/2 extensible leading-edge flaps.

Figure 6.- Continued.

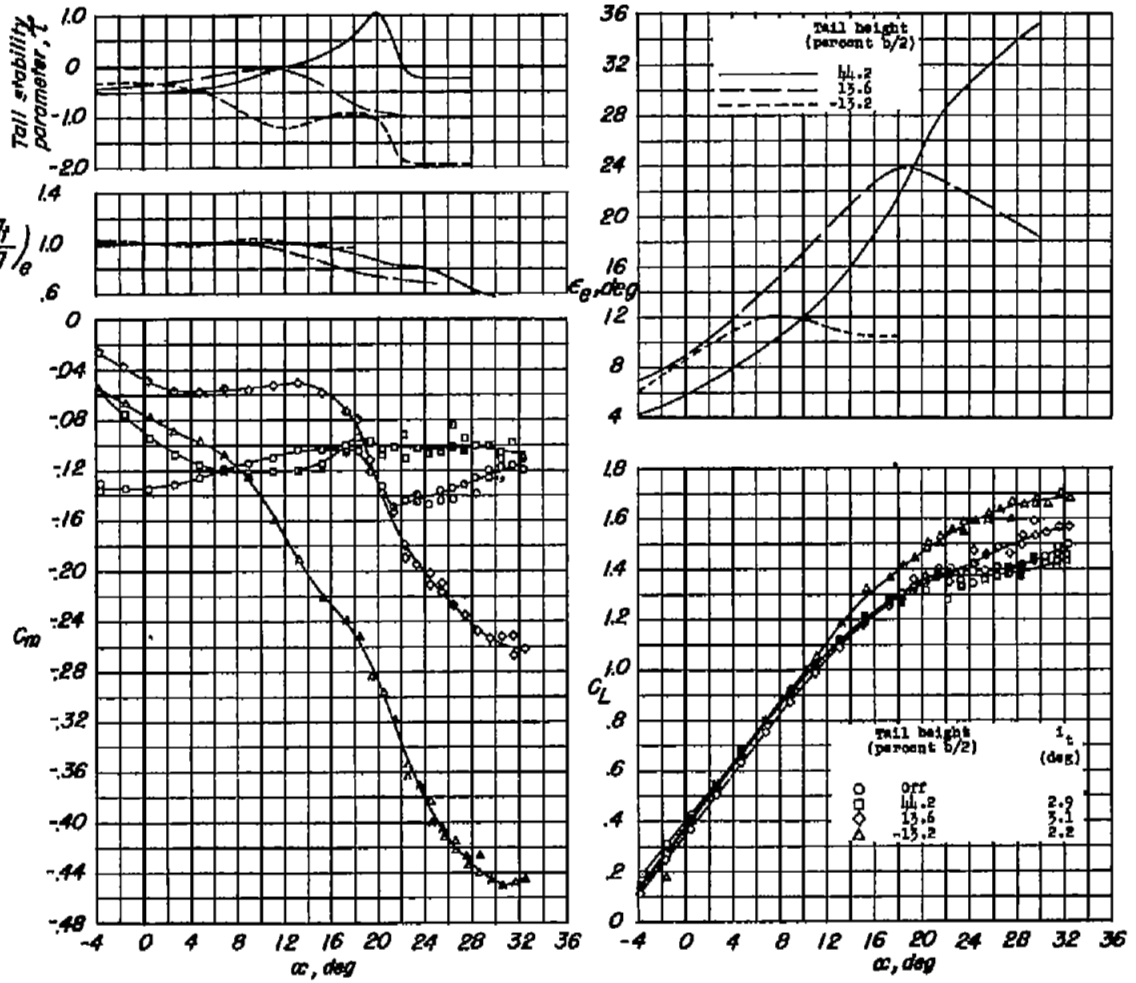

(c) Wing configuration, 0.25b/2 extensible leading-edge flaps and 0.5b/2 extended trailing-edge flaps.

Figure 6.- Continued.

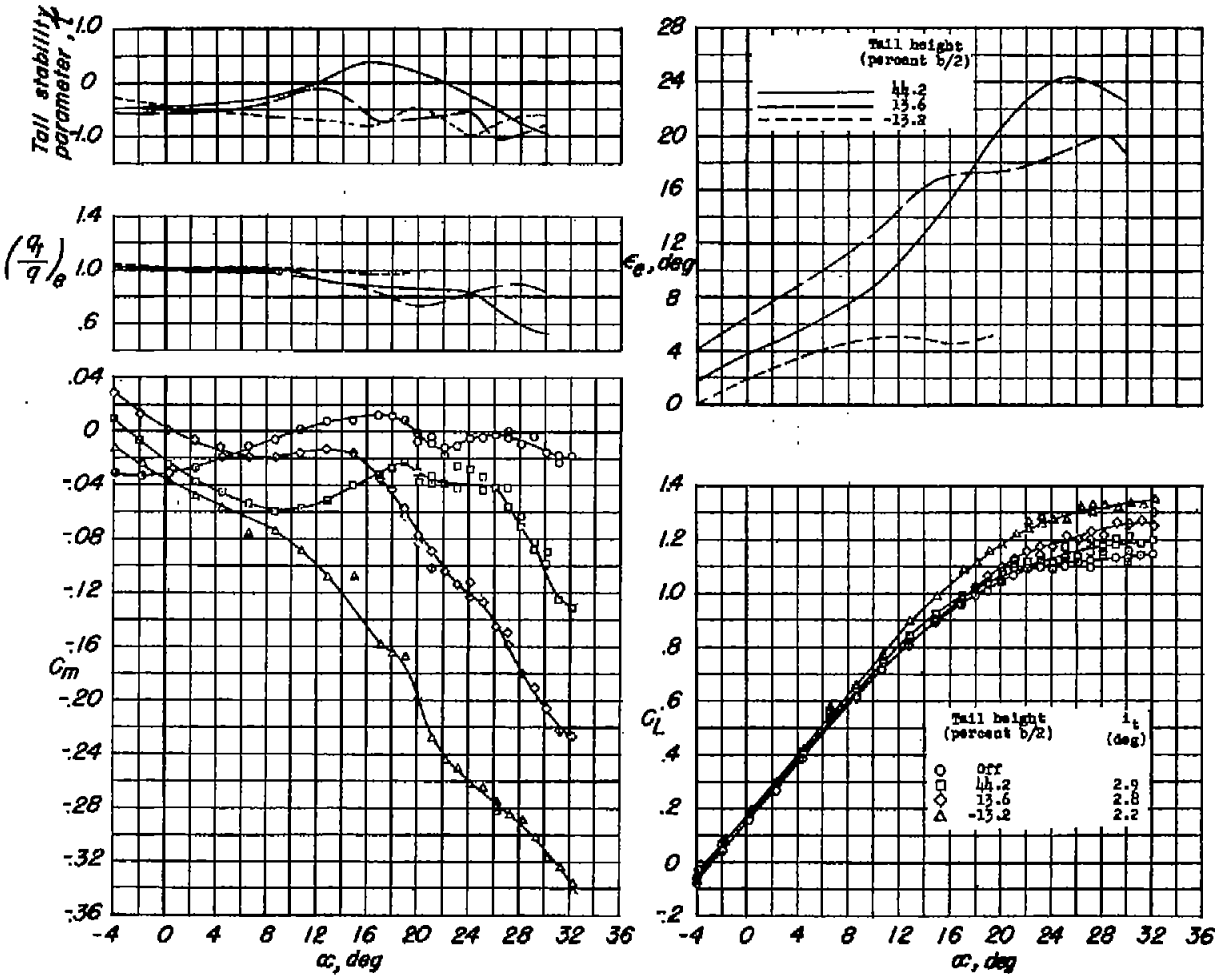

(d) Wing configuration, 0.25b/2 extensible leading-edge flaps and 0.40b/2 split flaps.

Figure 6.- Concluded.

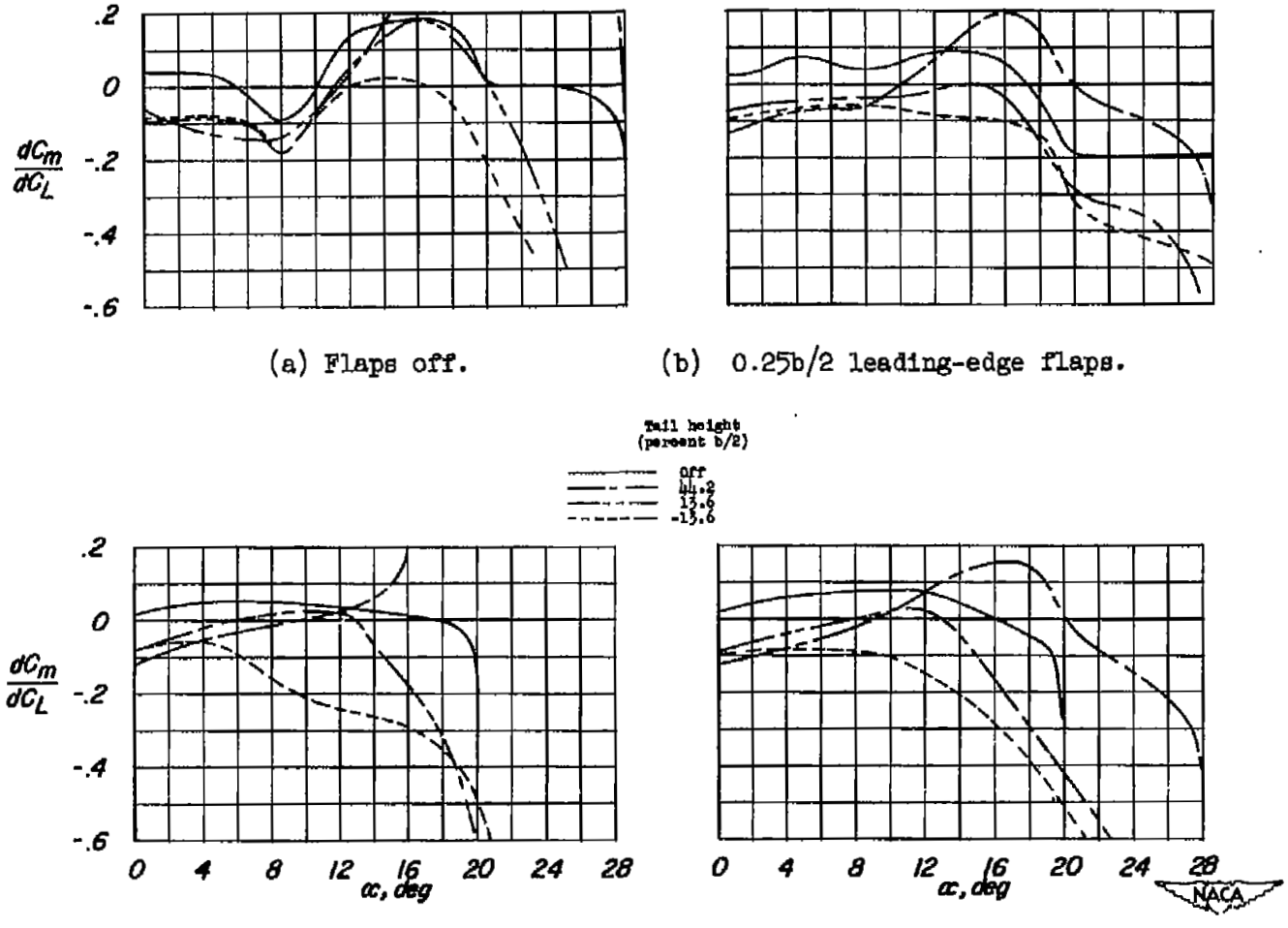

(a) Flaps off.

(b) 0.25b/2 leading-edge flaps.

(c) 0.25b/2 leading-edge flaps and 0.50b/2 extended trailing-edge flaps.

(d) 0.25b/2 leading-edge flaps and 0.40b/2 split flaps.

Figure 7.- Variation of dC_m/dC_L with angle of attack for various configurations of the wing-fuselage combination with and without the horizontal tail. $R = 5.5 \times 10^6$.

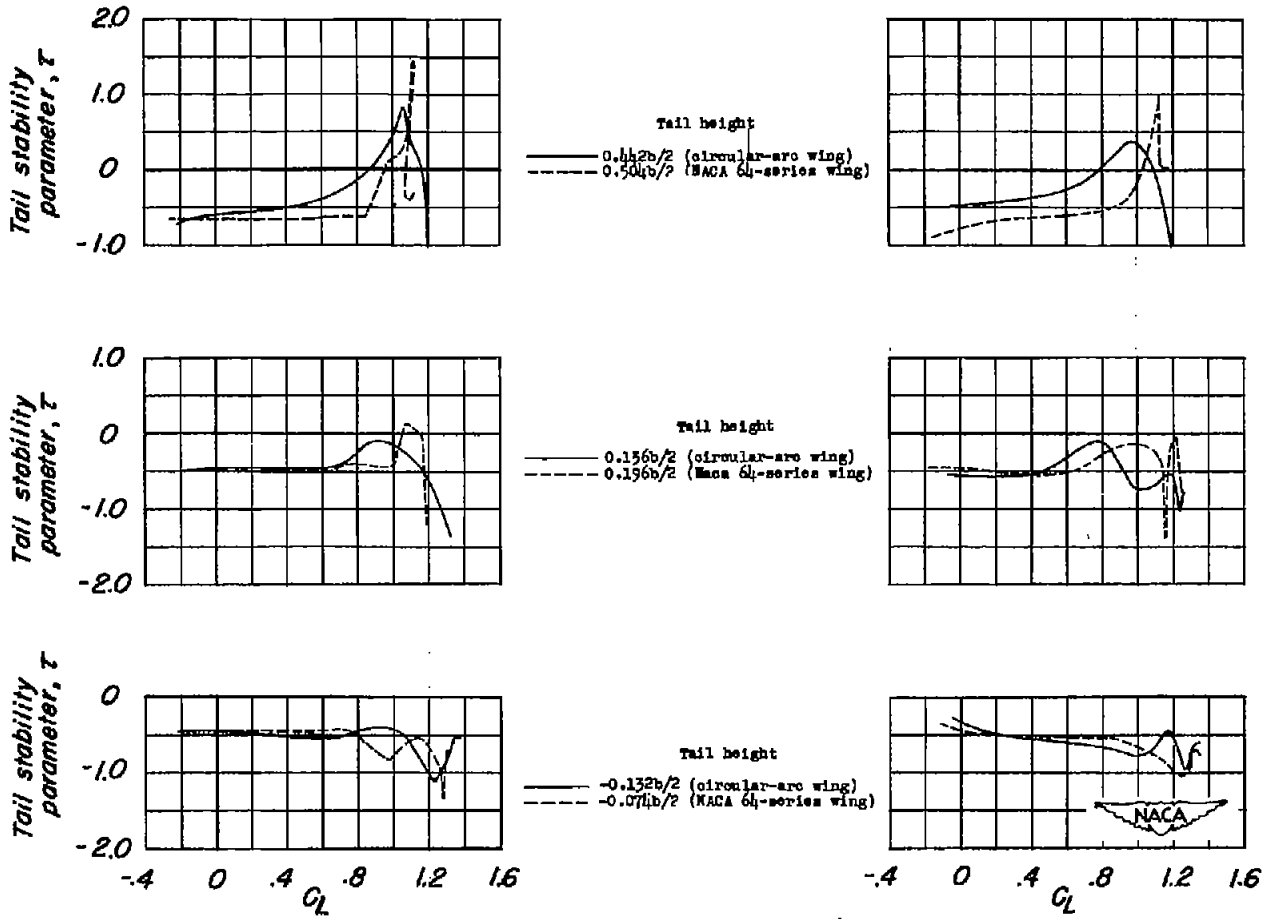

(a) Without flaps.

(b) With flaps.

Figure 8.- Comparison of the effectiveness of a horizontal tail in conjunction with a 52° sweptback circular-arc wing and with a 52° sweptback NACA 64-series wing (reference 6) with and without flaps. Circular-arc wing, 0.25b/2 leading-edge and 0.40b/2 split flaps; NACA 64-series wing, 0.40b/2 leading-edge and 0.40b/2 split flaps; aspect ratio approximately equal to 2.85.

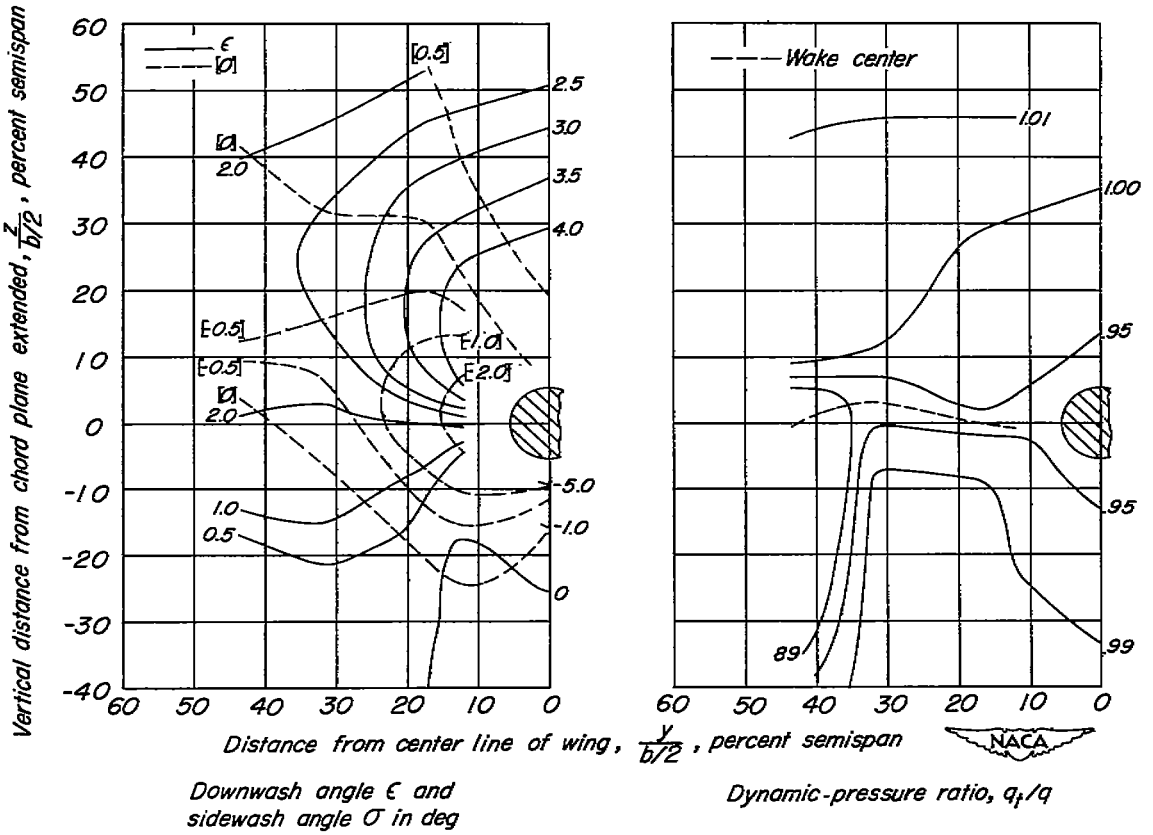

(a) $\alpha = 3.2^\circ$.

Figure 9.- Contours of downwash, sidewash, and dynamic-pressure ratio behind a 52° sweptback wing-fuselage in the region of a horizontal tail. Flaps off; $R = 5.5 \times 10^6$.

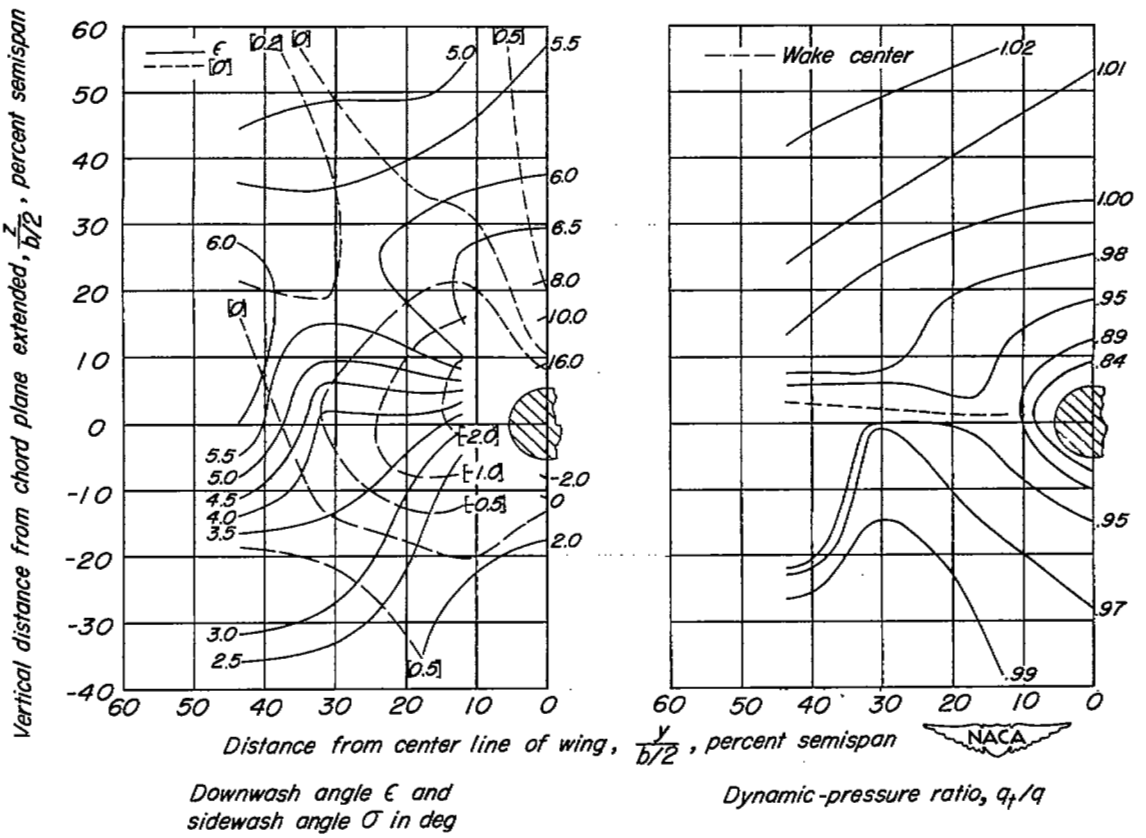

(b) $\alpha = 8.1^{\circ}$.

Figure 9.- Continued.

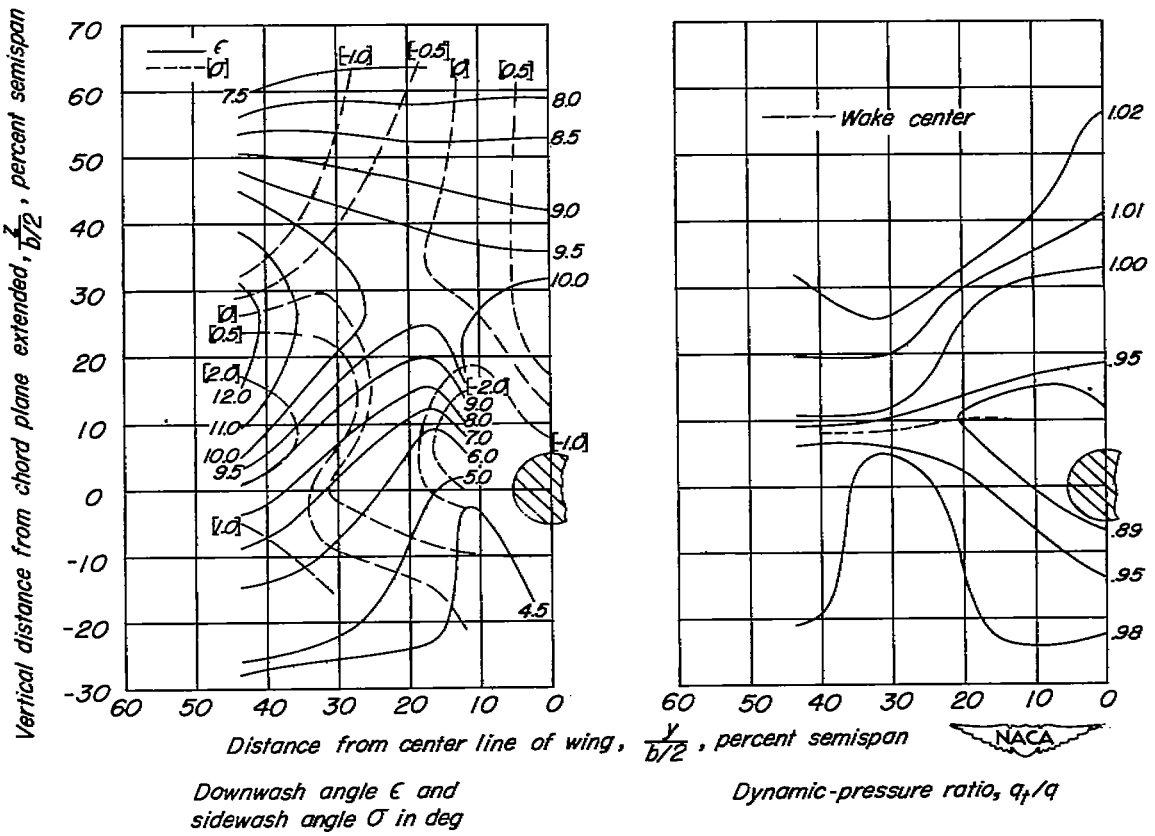

(c) $\alpha = 13.1^{\circ}$.

Figure 9.- Continued.

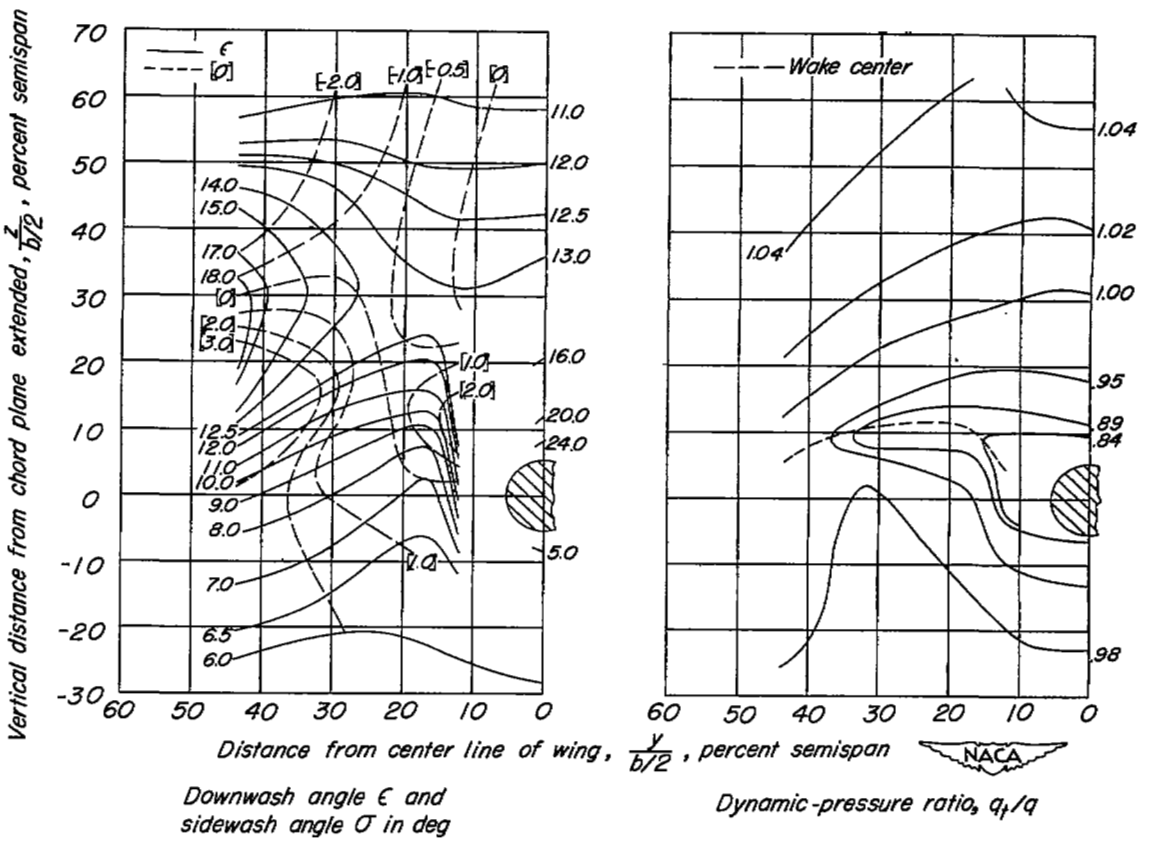

(d) $\alpha \approx 16.2^{\circ}$.

Figure 9.- Continued.

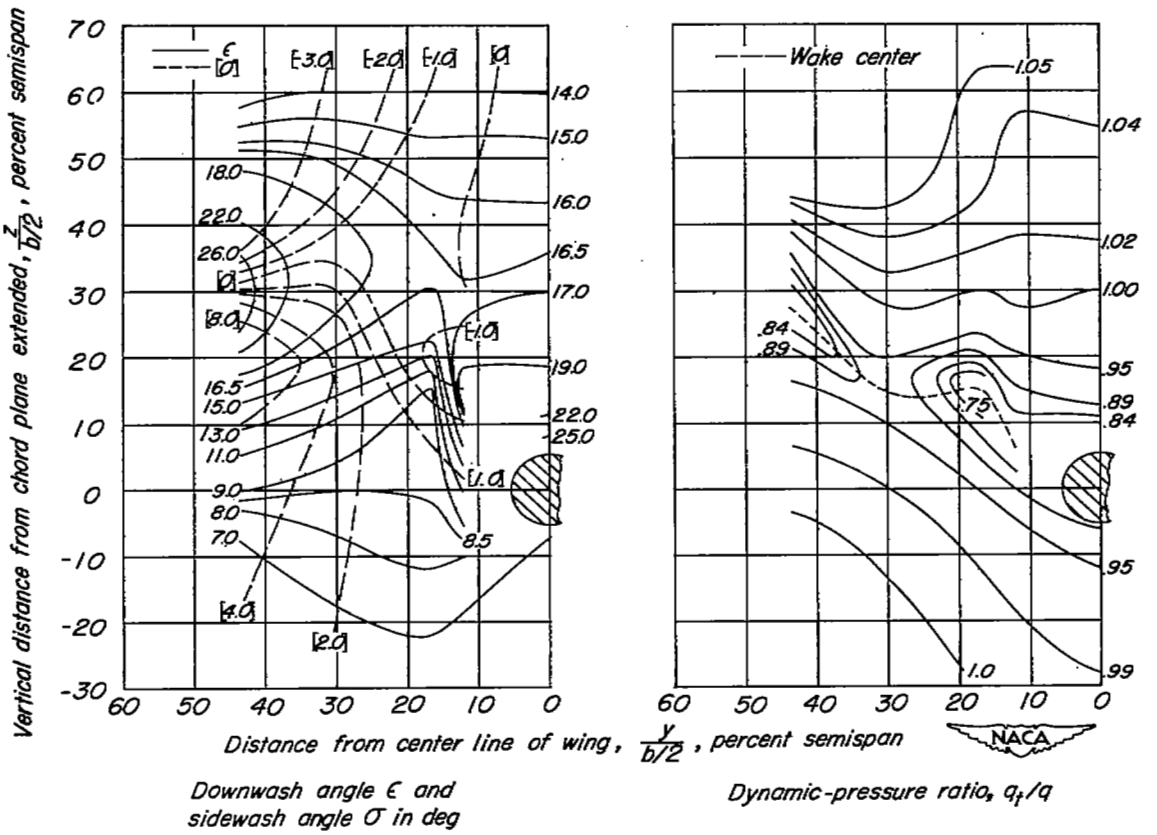

(e) $\alpha = 19.0^{\circ}$.

Figure 9.- Concluded.

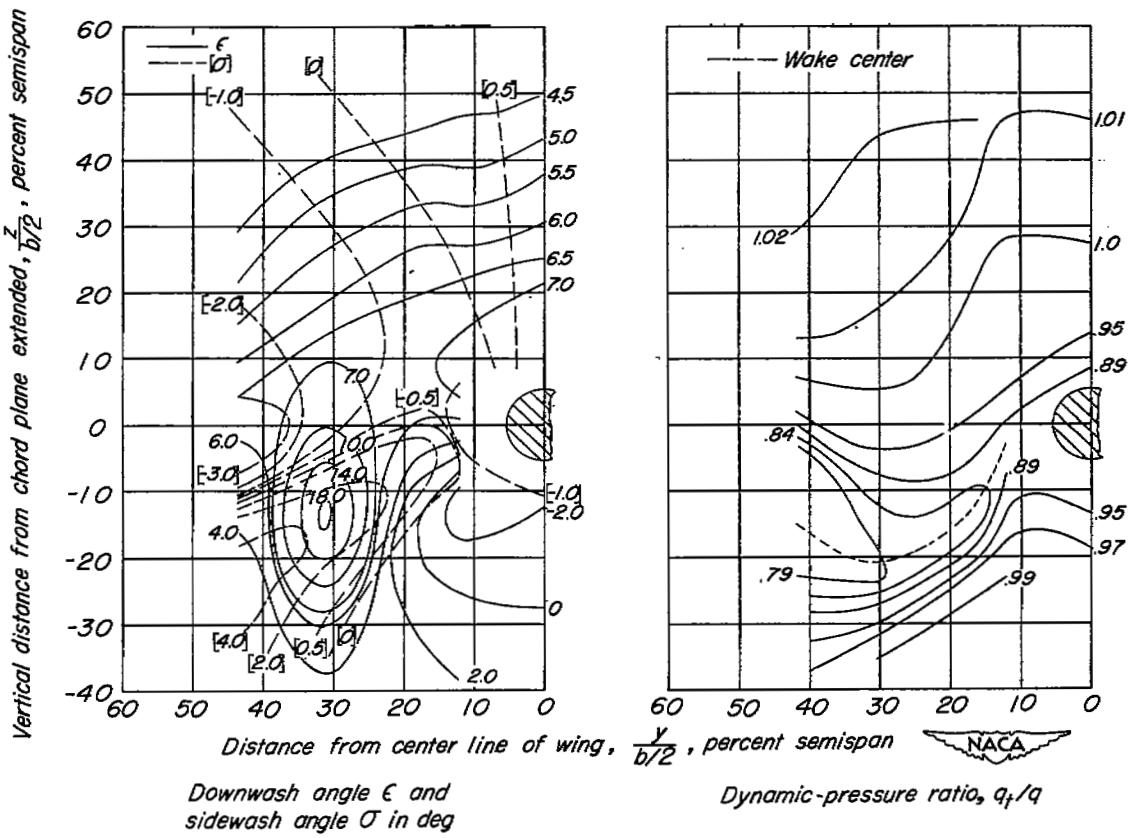

(a) $\alpha = 3.4^{\circ}$.

Figure 10.- Contours of downwash, sidewash, and dynamic-pressure ratio behind a 52° sweptback wing-fuselage in the region of a horizontal tail. 0.25b/2-span extensible leading-edge flaps; 0.4b/2-span split flaps; $R = 5.5 \times 10^6$.

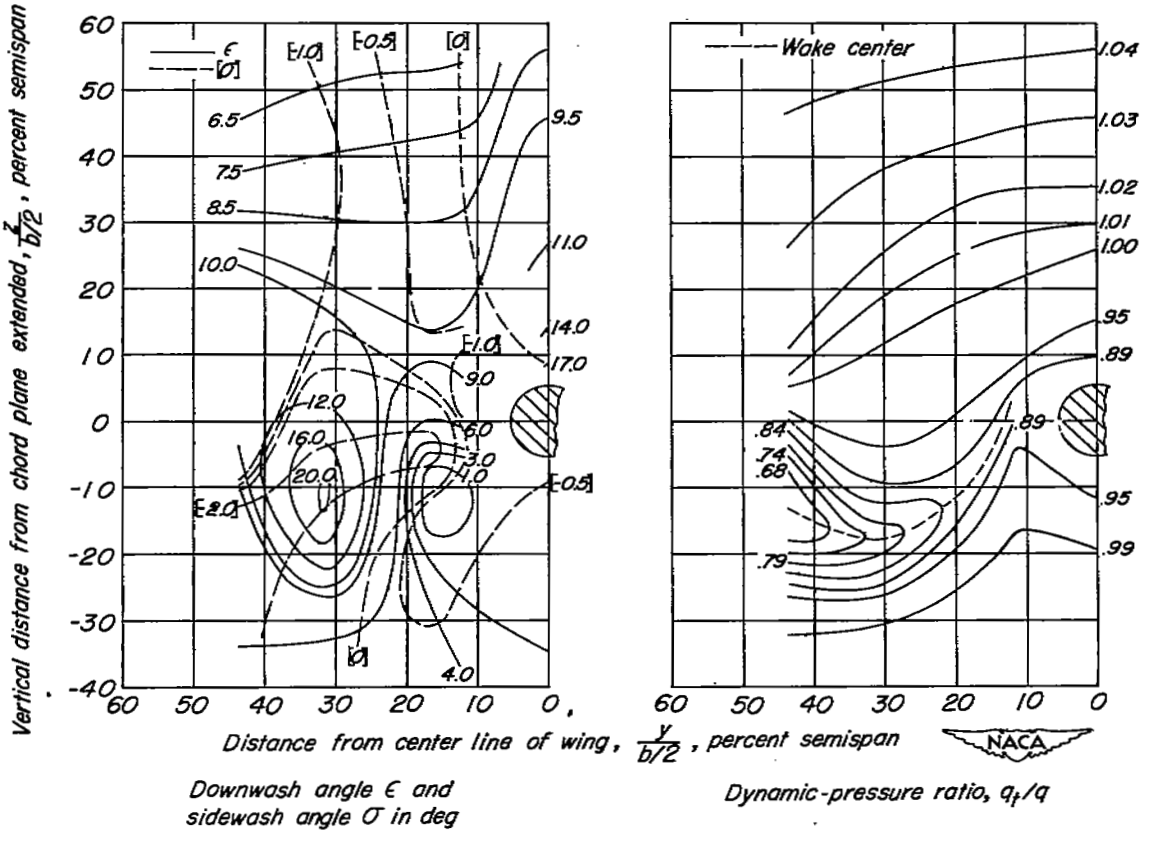

(b) $\alpha = 8.3^\circ$.

Figure 10.- Continued.

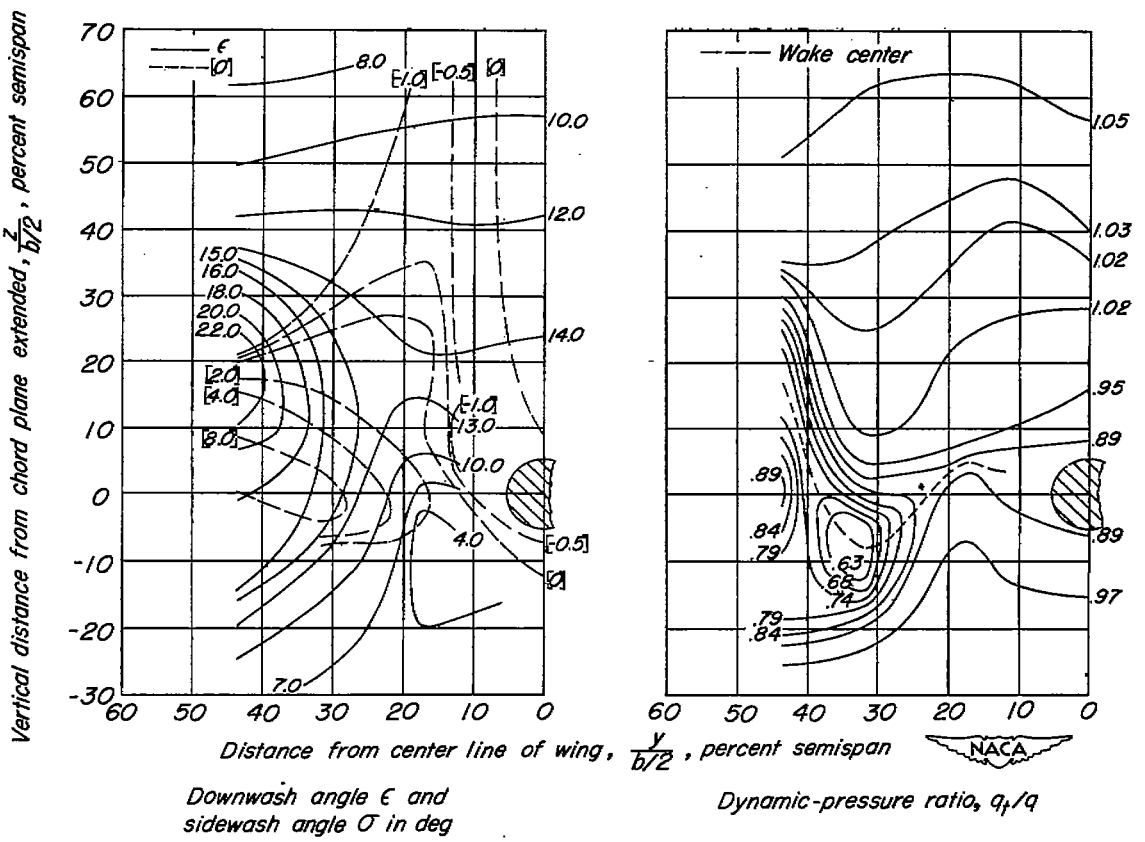

(c) $\alpha = 13.1^{\circ}$.

Figure 10.- Continued.

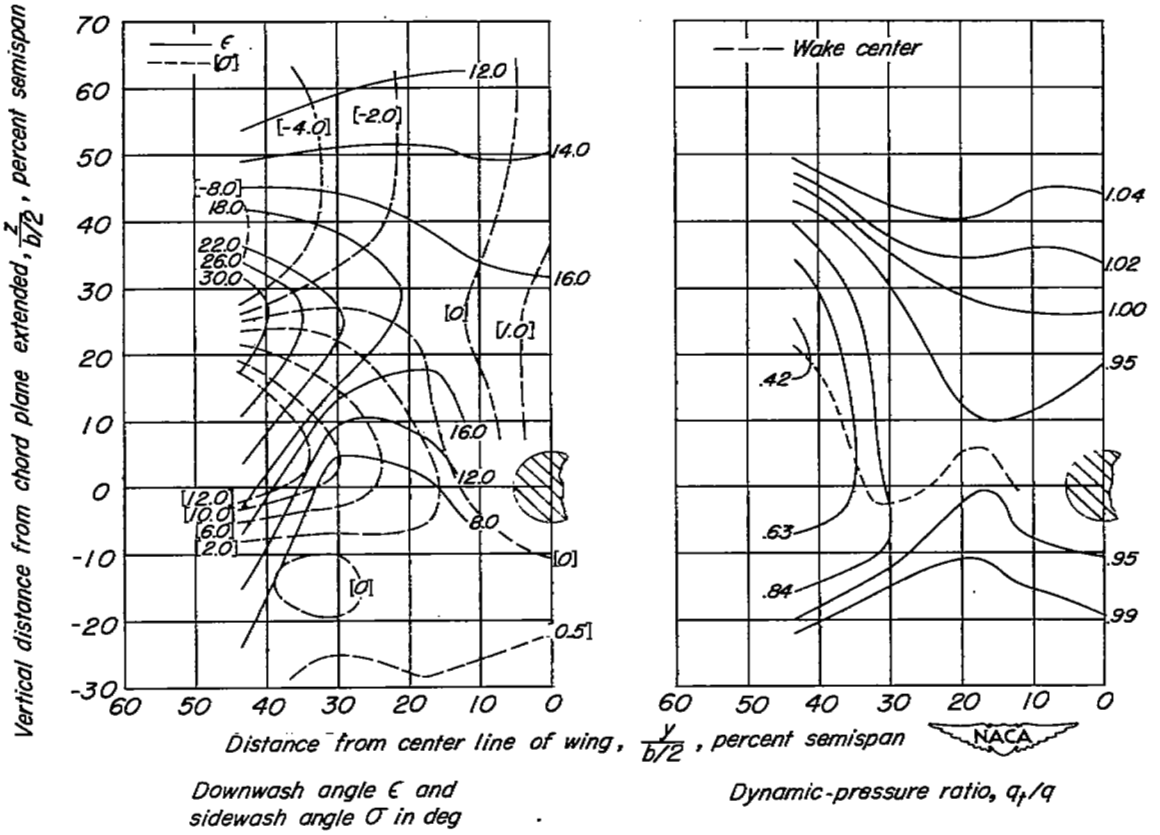

(d) $\alpha = 16.3^{\circ}$.

Figure 10.- Continued.

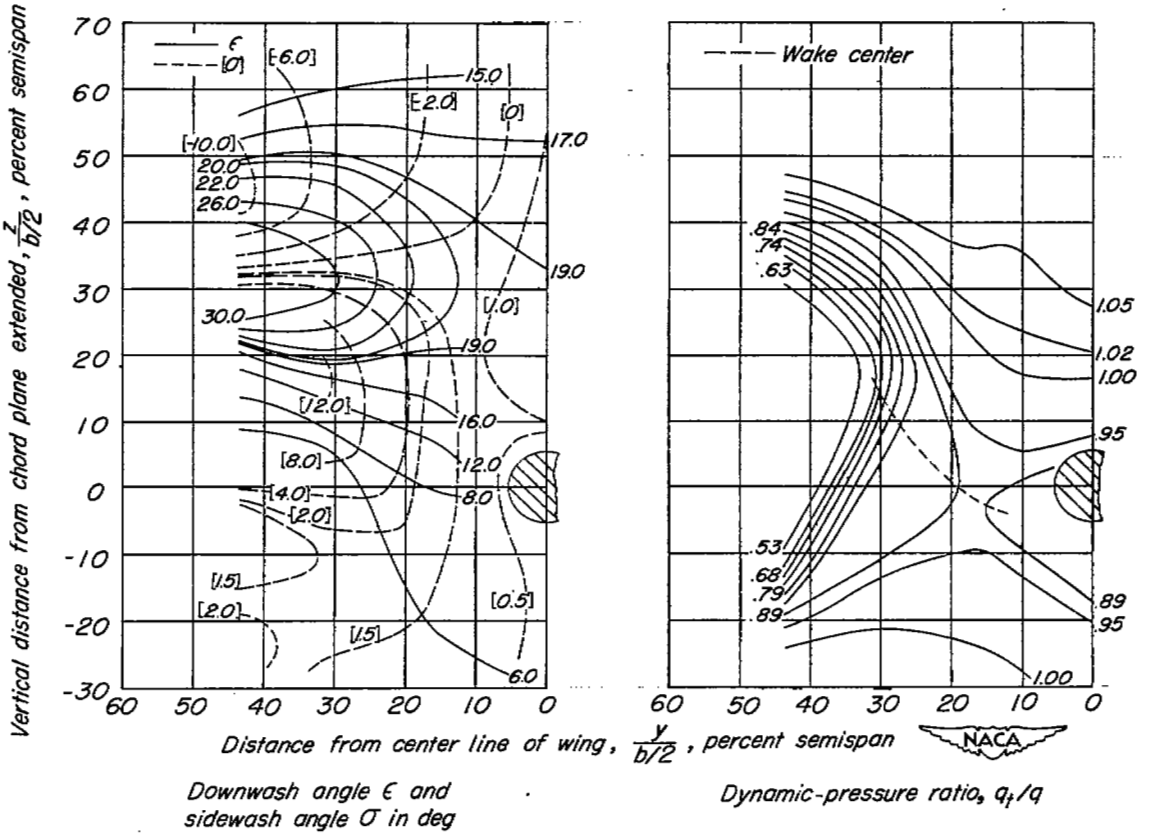

(e) $\alpha = 19.0^{\circ}$.

Figure 10.- Concluded.

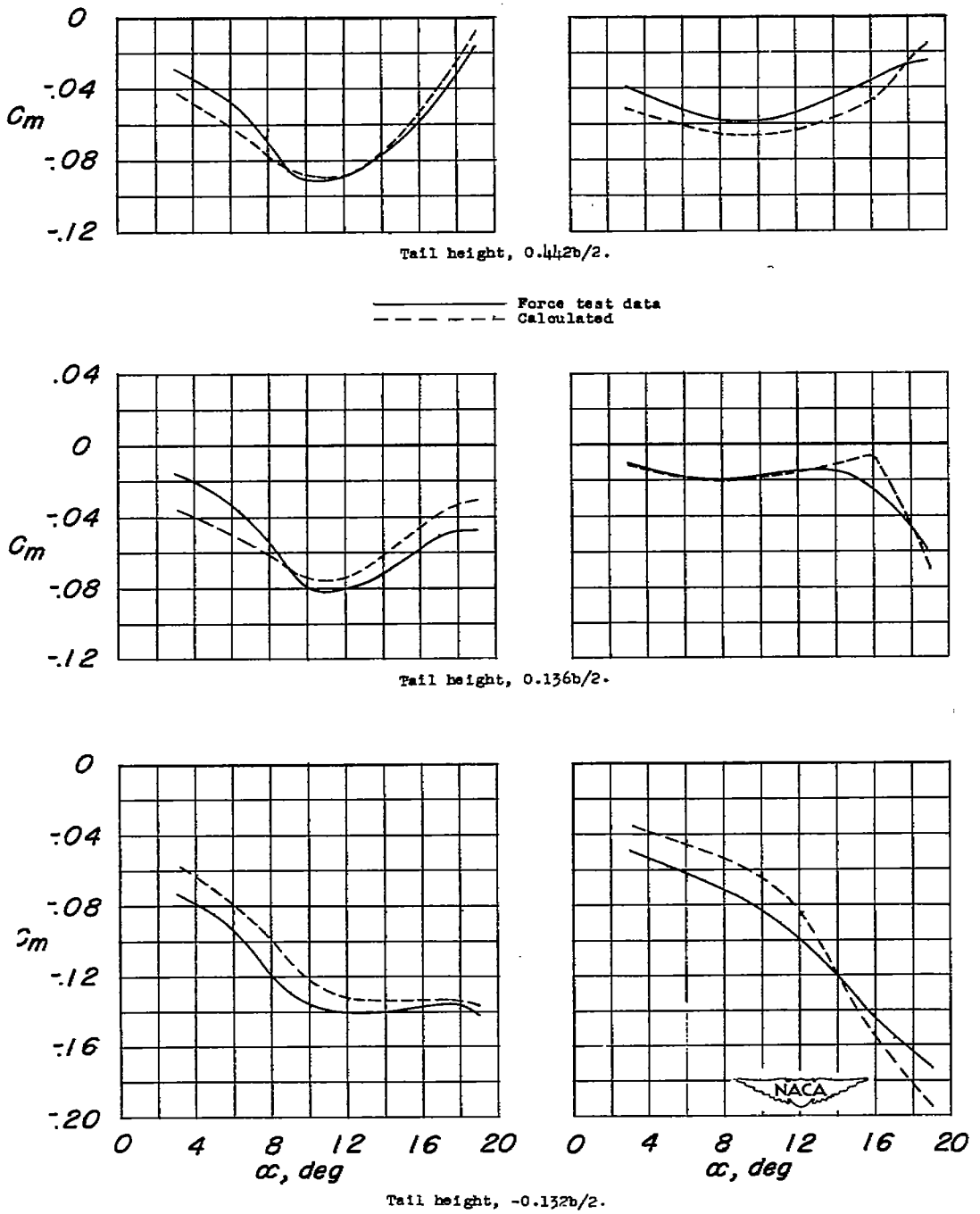

(a) Without flaps.

(b) With 0.25b/2 leading-edge and 0.40b/2 split trailing-edge flaps.

Figure 11.- Comparison of calculated and experimental pitching-moment coefficients of a 52° sweptback wing with and without flaps.

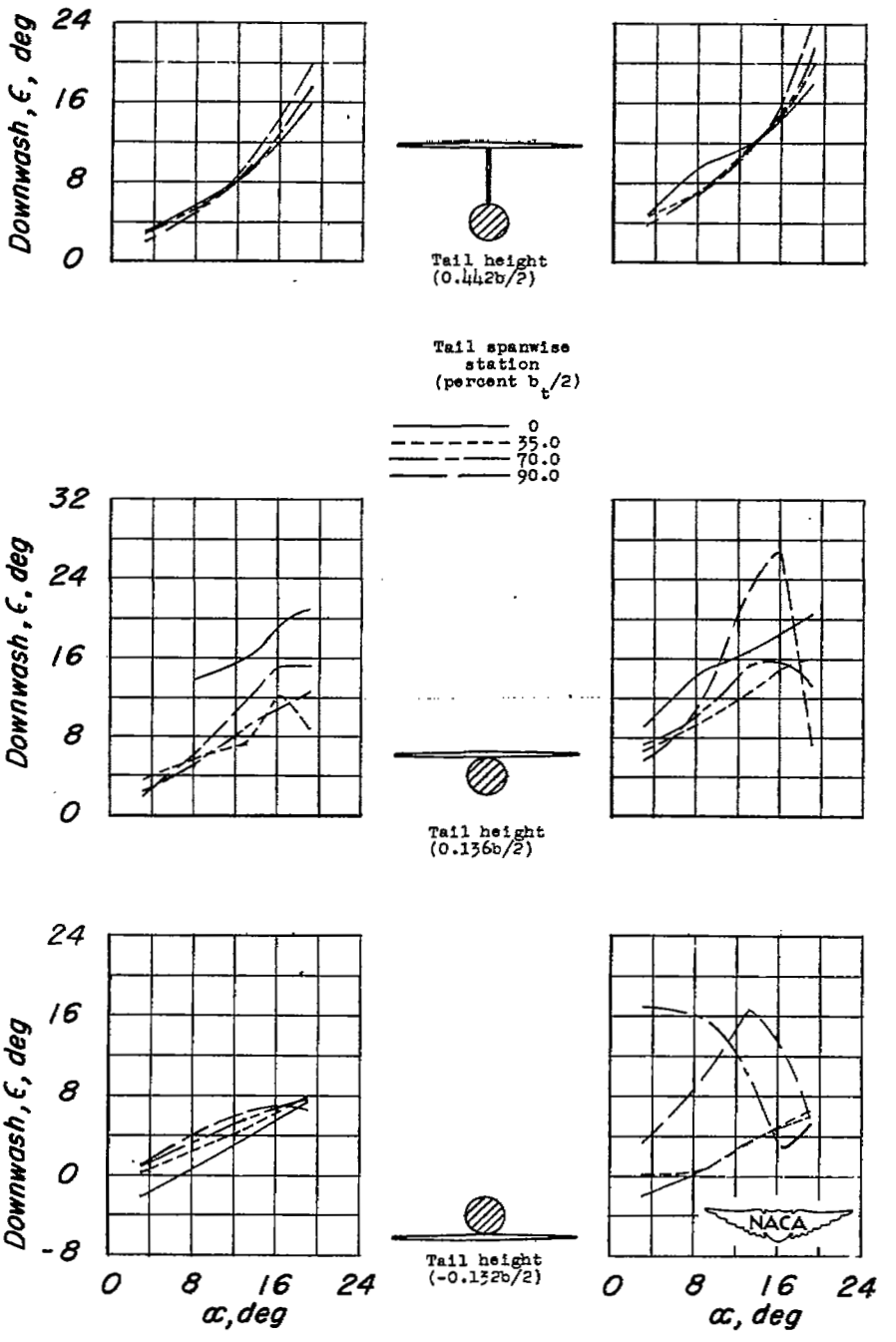

(a) Without flaps.

(b) With 0.25b/2 leading-edge and 0.40b/2 split trailing-edge flaps.

Figure 12.- Variation of downwash angle at several spanwise stations of various tail arrangements plotted against angle of attack.

NASA Technical Library
3 1176 01436 8550